*Electronic Supplementary Information*

# Thiosemicarbazone organocatalysis: tetrahydropyranylation and 2-deoxygalactosylation reactions and kinetics-based mechanistic investigation

Dennis Larsen,[‡] Line Malue Langhorn, Olivia Mulvad Akselsen, Bjarne Enrico Nielsen, and Michael Pittelkow

*Department of Chemistry, University of Copenhagen, Universitetsparken 5, DK-2100 Copenhagen, Denmark*

*‡ Current address: Department of Chemistry, Stanford University, Stanford, CA 94305, U.S.A.*
** Corresponding author: pittel@kiku.dk*

**Table of contents:**

# 1. General

### Chemicals and Instrumentation

Unless stated otherwise, all starting materials and solvents were purchased from commercial suppliers and used as received. HPLC grade solvents were used for synthesis and kinetics studies, and they were dried prior to use by standing over molecular sieves (4 Å). Water contents of dried solvents and reagents were measured on a Metrohm 737 KF coulometer. Melting points are uncorrected.

NMR spectra were recorded on a Bruker Ultrashield Plus 500 spectrometer, operating at 500 MHz ($^{1}$H) and 126 MHz ($^{13}$C). All $^{19}$F spectra, however, were recorded on an Oxford NMR 300 spectrometer, operating at 282 MHz. Unless specified otherwise all spectra were obtained at 20 °C and are referenced to the internal solvent residue for $^{1}$H and $^{13}$C, and to trifluoroacetic acid in a sealed tube for $^{19}$F. $CDCl_3$ was dried by standing over molecular sieves (4 Å) and treated with oven-dried basic aluminium oxide prior to use. Chemical shifts ($\delta$) are quoted in ppm and coupling constants (*J*) are listed in Hz. The following abbreviations are used for convenience in reporting the multiplicities of NMR resonances: s, singlet; d, doublet; t, triplet; q, quartet; m, multiplet; bs, broad singlet. The NMR data was processed using MestReNova v8.0.0 from MestreLab Research S.L. Assignment of $^{1}$H and $^{13}$C resonances was achieved using standard 1D and 2D NMR techniques; COSY, TOCSY, $^{13}$C-APT, HSQC ($^{1}$H and $^{13}$C) and HMBC ($^{1}$H and $^{13}$C).

### HPLC-UV and LC-MS:

HPLC analysis was performed on a Dionex UltiMate 3000 system, which incorporates an UltiMate 3000 diode array UV/Vis detector capable of measuring absorbance of light in the 190 – 800 nm range.

LC-MS analyses were carried out by connecting the above mentioned HPLC apparatus to a Bruker MicrOTOF-QII system equipped with an ESI source with nebulizer gas at 1.2 bar, dry gas at 10 L/min, dry temperature at 200 °C, capillary at 4500 V and end plate offset at −500 V. The ion transfer was conducted with funnel 1 and funnel RF's at 200.0 Vpp and hexapole RF at 100.0 Vpp while the quadrupole ion energy was set at 5.0 eV with a low mass cut-off at 100.00 m/z. In the collision cell, collision energy was set at 8.0 eV, collision RF at 100.0 Vpp, and a transfer time of 80.0 µs and pre-pulse storage of 1.0 µs were used.

Solvents and additives of LC-MS grade were purchased from commercial suppliers and used as received. Water was purified on a Millipore Milli-Q Integral 5 system. The mobile phase solutions prepared were: (A) 0.1 % formic acid in water and (B) 0.1 % formic acid in acetonitrile. Injection volumes were generally between 0.10 and 0.30 µL. The column was conditioned to the starting eluent with at least five column volumes prior to each injection. The gradient is outlined below:

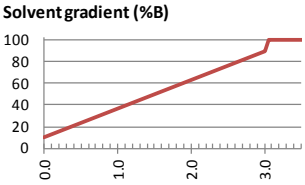


| Time (min) | %A | %B |
|---|---|---|
| **0.00** | 90 | 10 |
| **3.00** | 10 | 90 |
| **3.05** | 0 | 100 |
| **3.50** | 0 | 100 |
| **Flow-rate** | 1.000 mL/min | |

Separations were achieved using a Dionex Acclaim RSLC 120 C18 2.2 µm 120 Å 2.1×50 mm column maintained at 20 °C.

# 2. Optimisation of Reaction Conditions

An investigation to optimise the reaction conditions in order to achieve full conversion within a reasonable time frame was performed. First, a range of solvents was tested in combination with **DHP** (1:1 **DHP**/solvent) at 20 °C (external) using the best catalyst from the initial screening, namely catalyst **1b** (scheme 2.1).

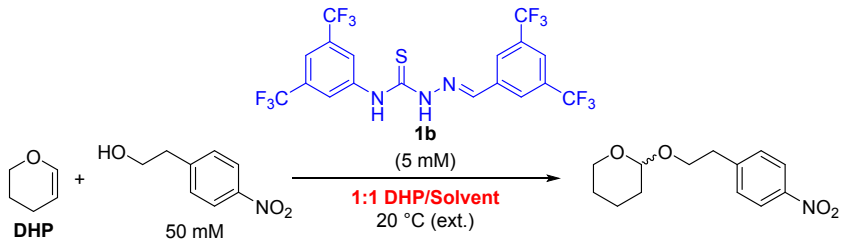


**Scheme 2.1:** Conditions used during solvent screening.

It was found that a wide range of solvents substantially reduced the reaction time, while also improving the conversion rates. Thus, several of the solvents resulted in improving the reaction rate so much that the reaction proceeded to afford full conversion within 48 hours or less (Table S1).

***Table S1: Solvent Screening***

| Solvent | Conversion[a] (time) | Solvent | Conversion[a] (time) |
|---|---|---|---|
| $CH_3NO_2$ | > 99 % (10 h)[b] | 1,4-Dioxane | 15 % (48 h) |
| $CH_2Cl_2$ | > 99 % (21 h) | 1,2-Dimethoxy ethane | 10 % (48 h) |
| $CS_2$ | > 99 % (28 h) | THF | 8.4 % (48 h) |
| Heptane | > 99 % (29 h) | DMF | < 1 % (48 h) |
| $CCl_4$ | > 99 % (31 h) | NMP | < 1 % (48 h) |
| Acetone | > 99 % (48 h) | DMSO | < 1 % (48 h) |
| Acetonitrile | 99 % (48 h) | Pyridine | < 1 % (48 h) |
| $CHCl_3$ | 94 % (48 h) | Piperidine | < 1 % (48 h) |
| Toluene | 89 % (48 h) | Tributyl amine | < 1 % (48 h) |
| 1,2-Dichloroethane | 87 % (48 h) | *N*,*N*-Diethylaniline | < 1 % (48 h) |
| Nitrobenzene | 87 % (48 h) | Benzonitrile | < 1 % (48 h) |
| Ethyl acetate | 28 % (48 h) | | |

Conditions as per scheme 2.1. [a] According to HPLC-UV at 290 nm (see below). [b] A significant amount of unidentified by-products were formed.

Most notably, $CH_2Cl_2$ afforded full conversion in 21 hours and in nitromethane the starting material was consumed in approximately 10 hours, albeit with a notable increase in by-product formation (as evidenced in the chromatograms by lower total area of the product peak as well as emergence of several peaks from unidentified by-products).

Overall the reaction proceeds well in non-polar solvents while the most polar solvents (DMSO, NMP, DMF) and solvents bearing alkaline nitrogen atoms (pyridine, tributyl amine, *N*,*N*-diethylaniline) inhibit the reaction completely. Combinations of nitromethane and $CHCl_3$ or $CH_2Cl_2$ were tested, but even though the conversion rate was indeed increased in these mixtures, by-products invariably formed even when as little as 5 vol-% nitromethane was used.

Based on these results it was decided to see how catalyst **1b** performed in $CH_2Cl_2$ when only 10 equivalents of **DHP** was added (scheme 2.2).

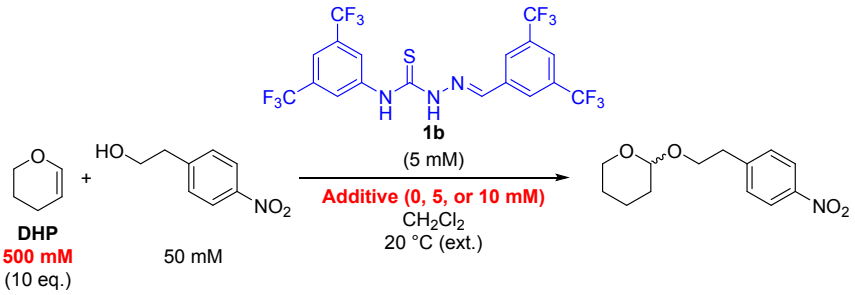


**Scheme 2.2:** Optimisation of concentrations and additives.

Gratifyingly, it was found that the reaction did take place even with a lower reactant loading, although full conversion of the alcohol was quite slow. Thus, approximately 100 hours at 20 °C was needed to afford full conversion (dashed red line in Figure S 1).

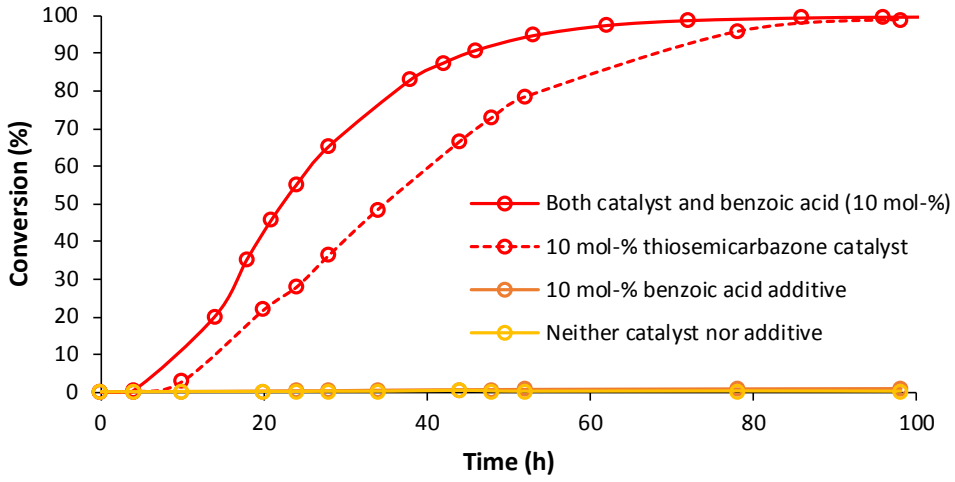


**Figure S 1:** Conversion profiles based on HPLC-UV at 290 nm. Conditions as per scheme 2.2. Data points represented by circles. Lines are merely to guide the eye.

Because of the slow conversion, benzoic acid was added (10 mol-%) to a range of reactions with and without catalyst **1b** to see if the reaction rate would be improved by the presence of a proton source. It was found that addition of benzoic acid gave a ca. 1.5-fold rate increase (see Table S2), but also that the reaction only takes place in presence of catalyst **1b**, as no considerable background product formation was observed when benzoic acid (10 mol-%) was used alone (orange line in figure s **1**).

The reaction was conveniently monitored by HPLC-UV at 290 nm, and the total area under the peaks for starting material and product remained constant during the reaction (figure s **2**). The wavelength of maximum absorbance, $\lambda_{max}$, was 279 nm for both starting material and product. These results underline that no significant changes in the absorption characteristics of the nitrophenyl UV marker occurs during the reaction.

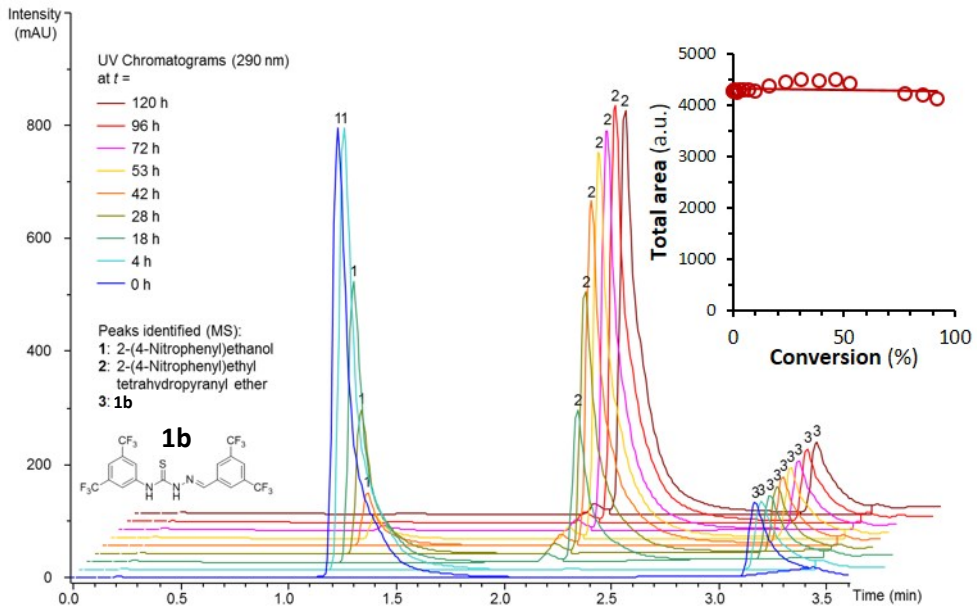


**Figure S 2:** UV chromatograms taken at different times during the reaction according to scheme 2.2 (with 5 mM benzoic acid). Inset shows the total area as a function of conversion percentage.

In conclusion, it was decided that conditions employing 10 mol-% thiosemicarbazone catalyst, 10 mol % benzoic acid and 10 eq. of DHP in $CH_2Cl_2$ at 20 °C were suitable for evaluating the catalytic efficacy of different thiosemicarbazone catalysts.

# 3. Kinetics Studies

## Procedure: Thiosemicarbazone-Catalysed Tetrahydropyranylation

Reactions were started by mixing freshly prepared stock solutions of the reactants and catalyst(s) in the appropriate solvent. Screw cap glass vials, of either 1.5 or 2.0 mL total volume, with PTFE lined septa where used as reaction vessels and the reactions were followed by LC-MS. All starting materials and products were identified by MS in order to determine their retention times.

The temperature was maintained by placing the samples in appropriately sized holes in a pre-tempered aluminium block in a thermostatically controlled auto sampler, and no stirring was applied. The time of analysis was calculated down to the minute using the time of injection registered by the apparatus. For reactions performed in volatile solvents (chloroform, dichloromethane etc.), the screw caps were exchanged after every injection to prevent excessive evaporation of solvent.

## Optimization of Catalyst

The reactions were conducted according to the optimized conditions identified above, followed by HPLC-UV at 290 nm (scheme 3.1), and data were fitted to a second-order reaction model using non-linear regression (see equation below) in order to obtain second order rate constants ($k_2$).

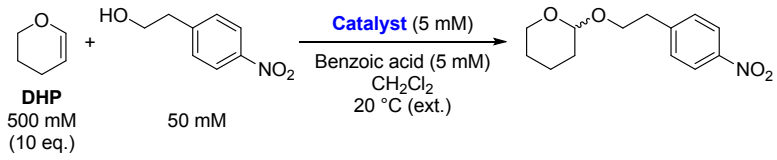


**Scheme 3.1:** Optimized conditions used for the catalyst optimization studies.

It was noted that under these conditions there was a significant time lag between preparation of the sample and the start of the reaction. This induction time, $t_i$, was taken into account in the second-order function by fitting to $(t - t_i)$ instead of $t$. Assuming first order dependence on both the alcohol and **DHP**, the concentration of product $[P]_{t_i}$ as a function of $(t - t_i)$ can be expressed by the starting concentrations of the alcohol, $[Alc]_0$, and **DHP**, $[DHP]_0$, and $k_2$:

$$[P]_{t_i} = \frac{[Alc]_0 \cdot e^{([Alc]_0 - [DHP]_0)k_2(t - t_i)} - [Alc]_0}{\frac{[Alc]_0}{[DHP]_0} \cdot e^{([Alc]_0 - [DHP]_0)k_2(t - t_i)} - 1}$$

Thus plotting the product concentration as a function of time, $[P]_{t_i}$, allows the use of non-linear regression to determine $t_i$ and $k_2$ (see below for a full elucidation of this equation).

A plot of the conversion over the first 100 hours using the catalysts listed in Table S2 is shown in figure s **3** (left). An illustrative example of data fitting for catalyst **1b** is also found in figure s **3** (right).

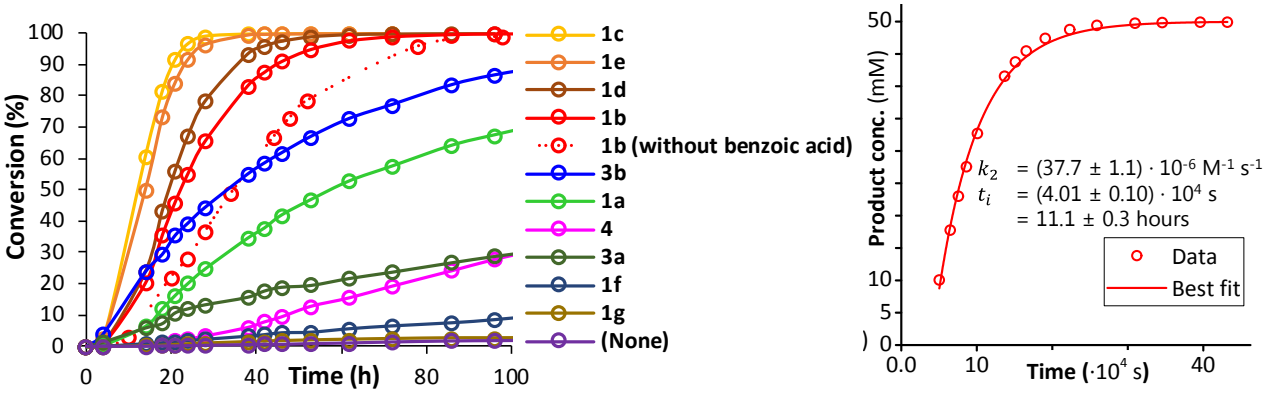


**Figure S 3: Left:** Conversion profiles (HPLC-UV at 290 nm) for the first 100 hours of reaction with ten of the catalysts in Table S2 (the thiosemicarbazides **1** and **3** are omitted due to side-reactions). Conditions as per scheme 3.1. Data points represented by circles. Lines are merely to guide the eye. **Right:** Using data for catalyst **1b**, shown are data points (o), best fit (–), and parameters obtained from fit to the equation for second-order reactions presented in this section. Note the time axis unit has been switched to seconds in order to obtain the rate constants in units of seconds as well.

***Table S2: Catalyst Optimization***

| | Catalyst | $t_i$ (h) | $k_2$[a] | | Catalyst | $t_i$ (h) | $k_2$[a] |
|---|---|---|---|---|---|---|---|
| **1** | 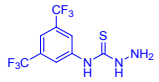 | *c.n.d.* | *c.n.d.* | **1f** | 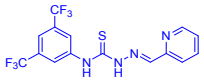 | *c.n.d.* | *c.n.d.* |
| **1a** | 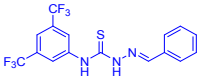 | 4.0 ± 1.4 | 6.8 ± 0.2 | **1g** | 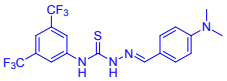 | *c.n.d.* | *c.n.d.* |
| **1b** | 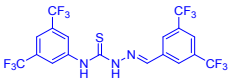 | 11.1 ± 0.3 | 37.7 ± 1.1 | **1h** | 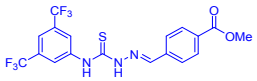 | *c.n.d.* | *c.n.d.* |
| **1b** (without benzoic acid) | 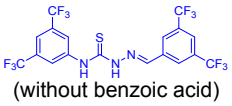 | 17.4 ± 0.9 | 24.9 ± 1.4 | **3** | 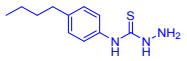 | *c.n.d.* | *c.n.d.* |
| **1c** | 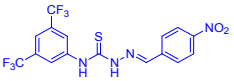 | 9.9 ± 0.2 | 129 ± 5 | **3a** | 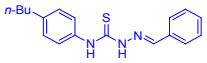 | 0[b] | 1.83 ± 0.05 |
| **1d** | 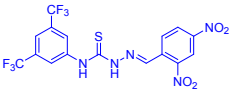 | 11.5 ± 0.3 | 53 ± 2 | **3b** | 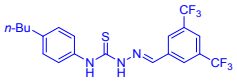 | 1.51 ± 0.19 | 12.38 ± 0.07 |
| **1e** | 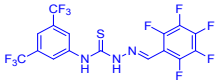 | 10.14 ± 0.16 | 101 ± 3 | **4** | 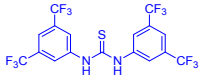 | 23.6 ± 1.3 | 2.55 ± 0.03 |

Conditions as per scheme 3.1. [a] All values in units of $10^{-6}$ $M^{-1}$ $s^{-1}$ with standard errors from fit to non-linear regression to the equation for second order reactions presented in this section. [b] In this case the best fit was obtained by setting $t_i$ to zero. *c.n.d.* could not be determined.

Attempts to use free thiosemicarbazides **1** and **3** as catalysts led to appreciable by-product formation in a matter of hours, and no product formation could be detected (Table S2). Thus, it must be the thiosemicarbazone itself acting as a catalyst, and not the free thiosemicarbazides that would result from hydrolysis *in situ*. No hydrolysis of any of the thiosemicarbazones were detected under the reaction conditions (HPLC-UV).

Catalyst **1f** and **1g** did not give enough turnover for proper quantification of the second order rate constant, though small amounts of product formation were detected (11 % and 2.7 % turnover (HPLC-UV), respectively, in 120 hours).

Measurements with catalyst **1h** had to be abandoned due to low solubility, which was evidenced by formation of a precipitate in the reaction vessels, as well as in stock solutions of the catalyst, within less than an hour of preparation.

The previously reported thiourea catalyst **4** gave relatively slow turnover under these dilute conditions. As is evident from the figure below, catalyst **4** gave only 73 % conversion over a prolonged period of 14 days, while catalyst **1c** gave full turnover in ca. 28 hours:

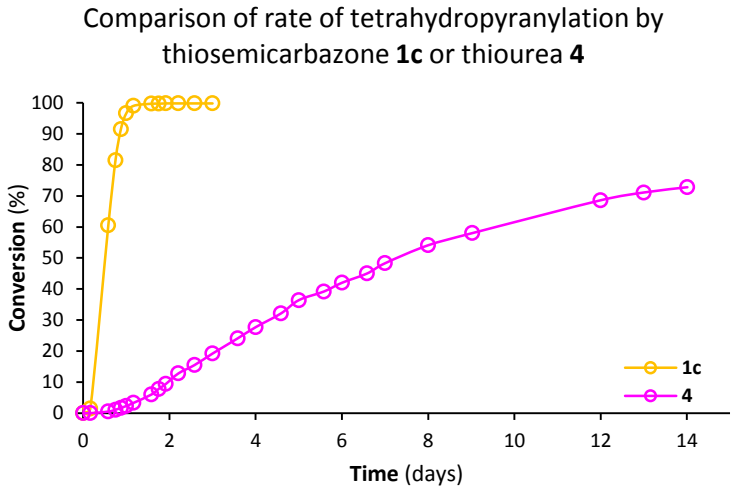

## Equation for Non-Linear Regression to Obtain Second-Order Rate Constants

The reaction between **DHP** and an alcohol, and the concentrations of starting materials and product at start of the reaction, during the reaction, and at the end of the reaction is expressed as follows:

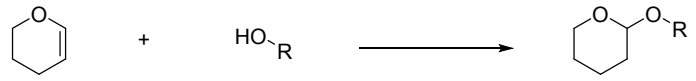


| | **DHP** | **Alc** | **P** |
|---|---|---|---|
| **Conc.:** | | | |
| **Start:** | $[DHP]_0$ | $[Alc]_0$ | 0 |
| ***t*:** | $[DHP]_t = [DHP]_0 - [P]_t$ | $[Alc]_t = [Alc]_0 - [P]_t$ | $[P]_t$ |
| **Final:** | $[DHP]_f = [DHP]_0 - [Alc]_0$ | $[Alc]_f = 0$ | $[P]_f = [Alc]_0$ |

The concentrations of alcohol and product is monitored by HPLC-UV (see below), and the concentration of **DHP** can be derived from those values.

For $[Alc]_0 \neq [DHP]_0$, the integrated second order rate law (assuming 1st order in both $[Alc]$ and $[DHP]$) can be written as:[1]

$$\frac{[Alc]_t}{[DHP]_t} = \frac{[Alc]_0}{[DHP]_0} \cdot e^{\left([Alc]_0 - [DHP]_0\right)k_2 t}$$

with $k_2$ being the second order rate constant.

Employing $[DHP]_t = [DHP]_0 - [P]_t$ and $[Alc]_t = [Alc]_0 - [P]_t$, and then rearranging to isolate $[P]_t$, one arrives at:

$$[P]_t = \frac{[Alc]_0 \cdot e^{\left([Alc]_0 - [DHP]_0\right)k_2 t} - [Alc]_0}{\frac{[Alc]_0}{[DHP]_0} \cdot e^{\left([Alc]_0 - [DHP]_0\right)k_2 t} - 1}$$

This equation assumes the reaction to start at $t_0$, however as this was found not to be the case, this equation fails to give acceptable fits when fitting the observed product concentration versus $t$. Therefore, the data was fitted as a function of $(t - t_i)$ in stead of $t$:

$$[P]_{t_i} = \frac{[Alc]_0 \cdot e^{\left([Alc]_0 - [DHP]_0\right)k_2 (t - t_i)} - [Alc]_0}{\frac{[Alc]_0}{[DHP]_0} \cdot e^{\left([Alc]_0 - [DHP]_0\right)k_2 (t - t_i)} - 1}$$

[1] P. Atkins and J. D. Paula, *Atkins' physical chemistry*, 8th edn., Oxford University Press, 2006.

## Representative UV Chromatograms and Time-Dependent Concentration Changes from Catalyst Screening with 2-(4-Nitrophenyl)ethanol

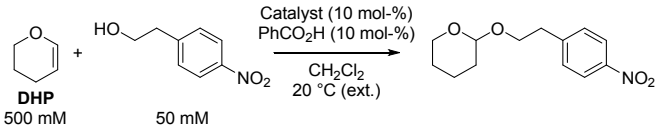


All reactions were performed with 2-(4-nitrophenyl)ethanol, which produce a distinct UV absorption signal at 290 nm. The THP-protected product has similar extinction coefficient (e.g. a response factor of 1), making the screening procedure with this alcohol very simple. Thus, the conversion percentage is simply the area of product divided by the total area of the product and the starting material.

### No catalyst:

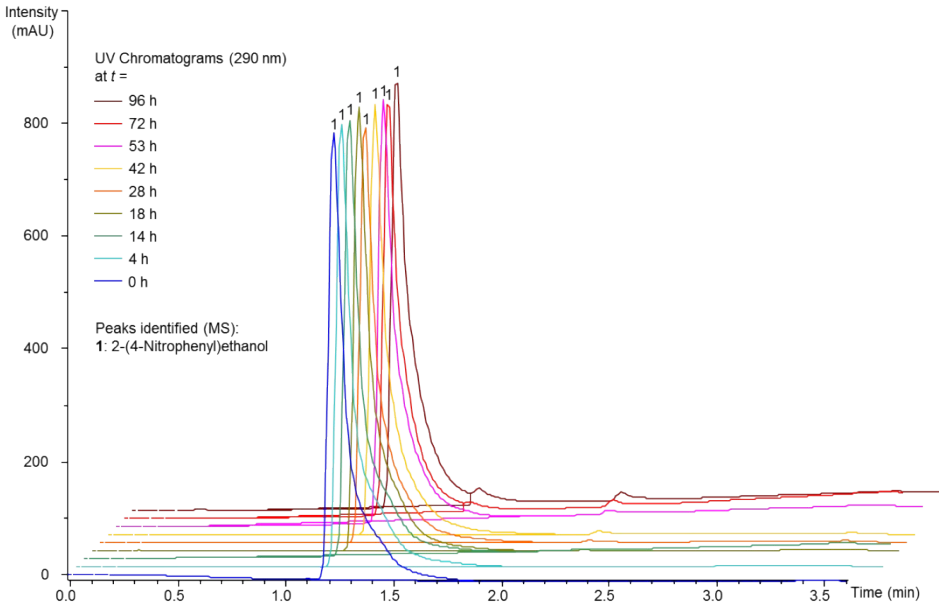


### Catalyst: 1

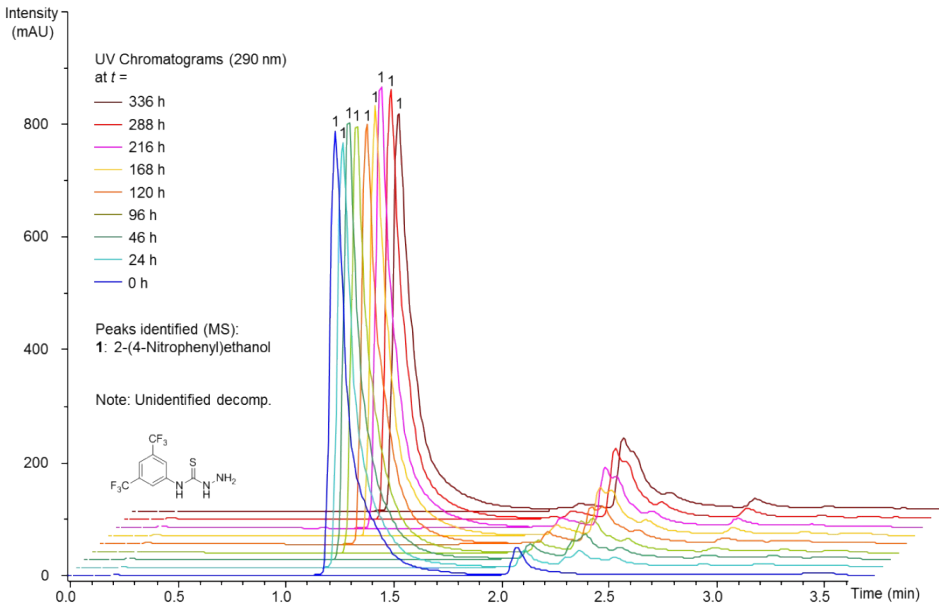

## Catalyst: 1a

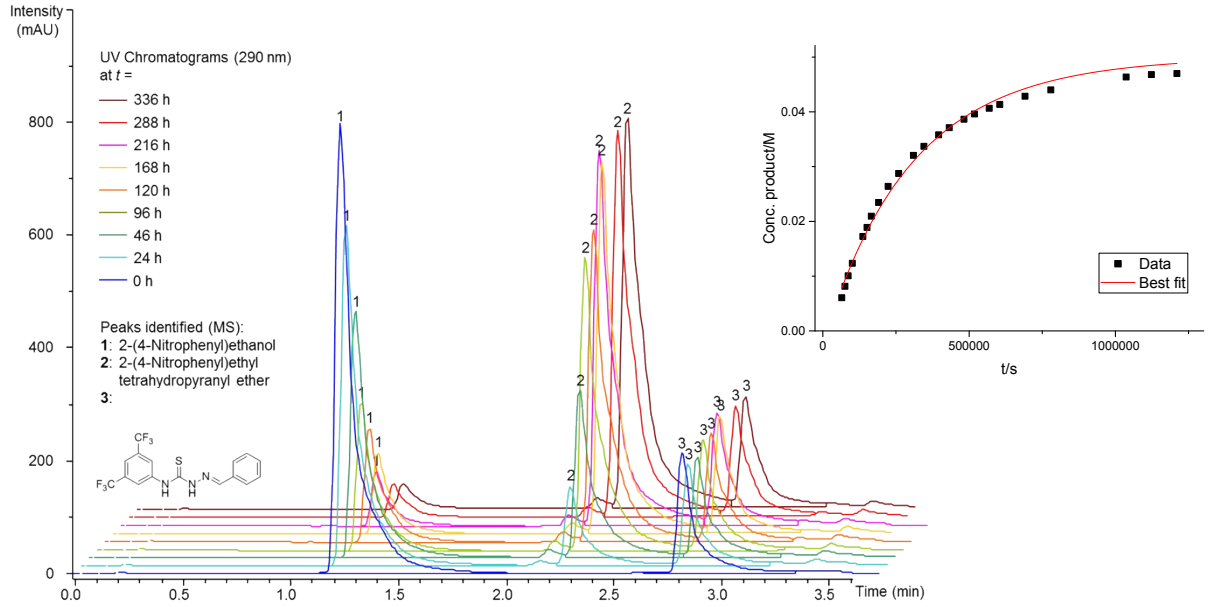


## Catalyst: 1b

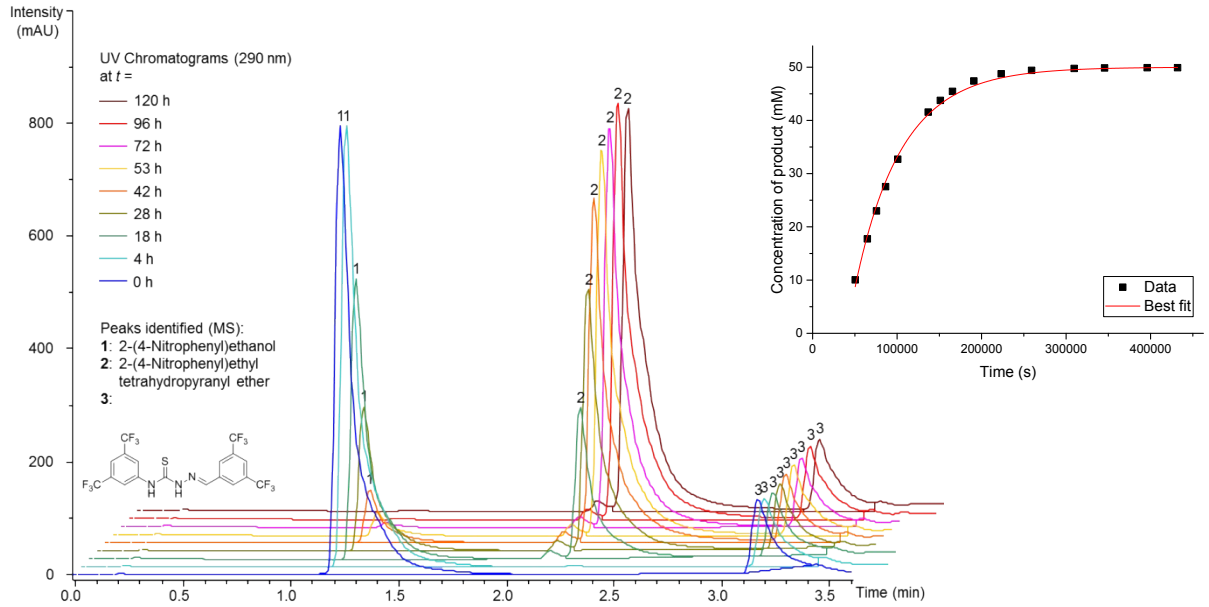

## Catalyst: 1c

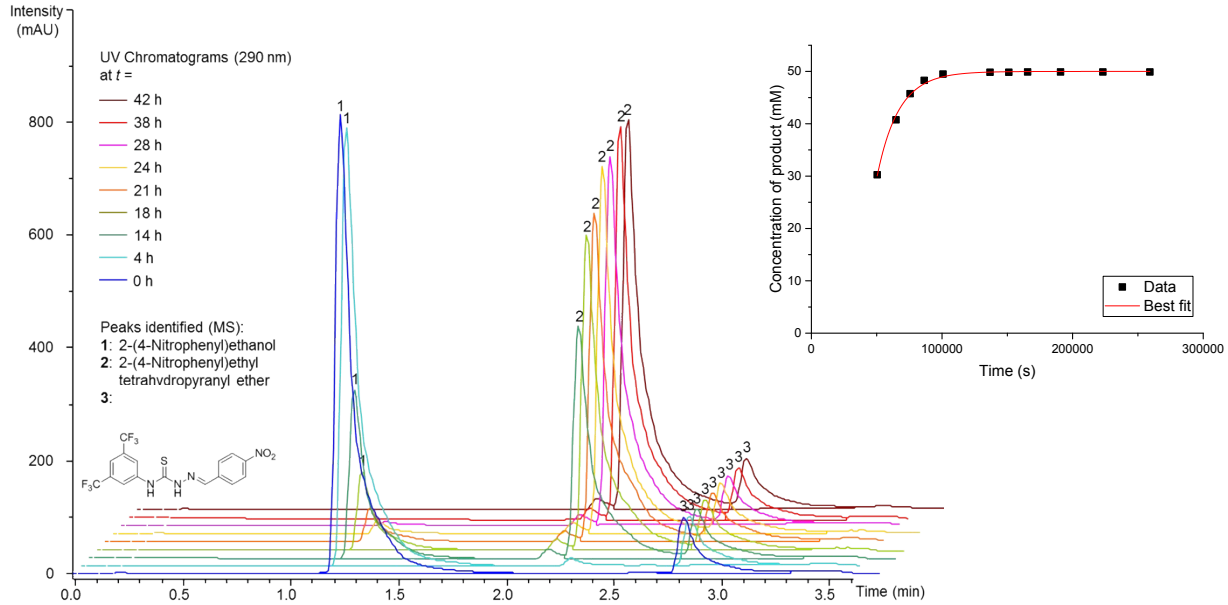


## Catalyst: 1d

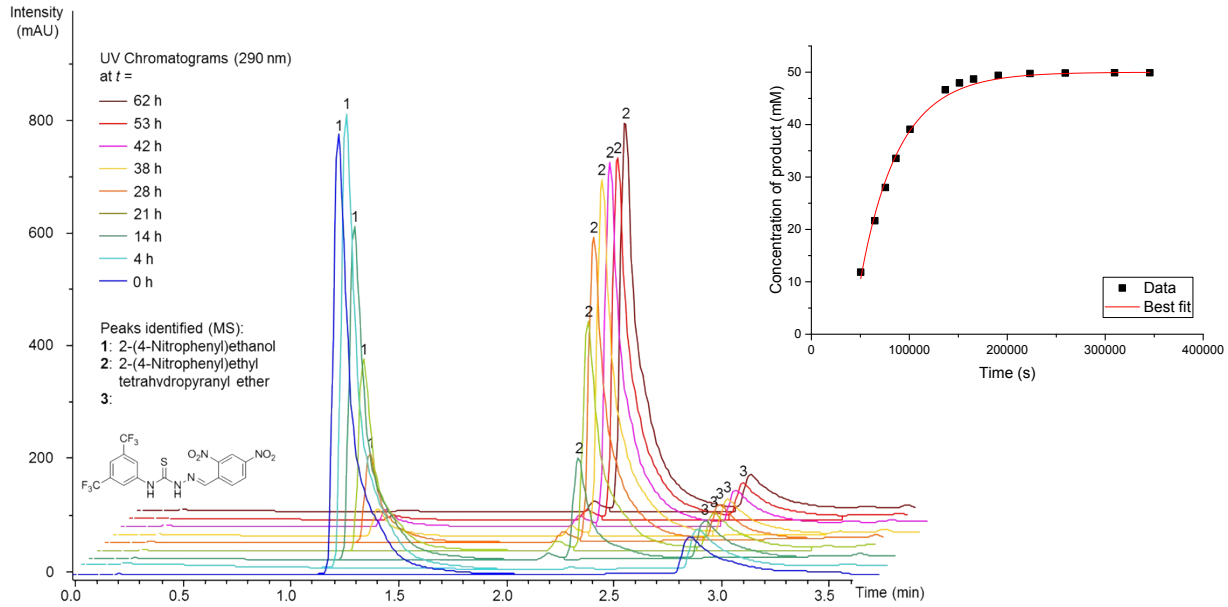

## Catalyst: 1e

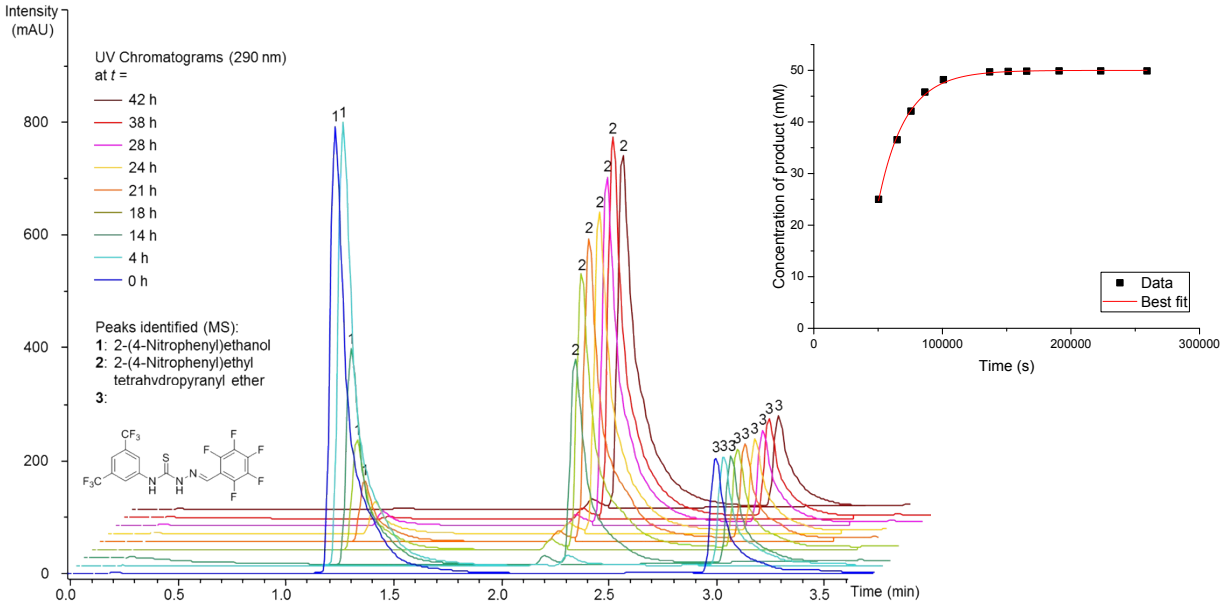


## Catalyst: 1g

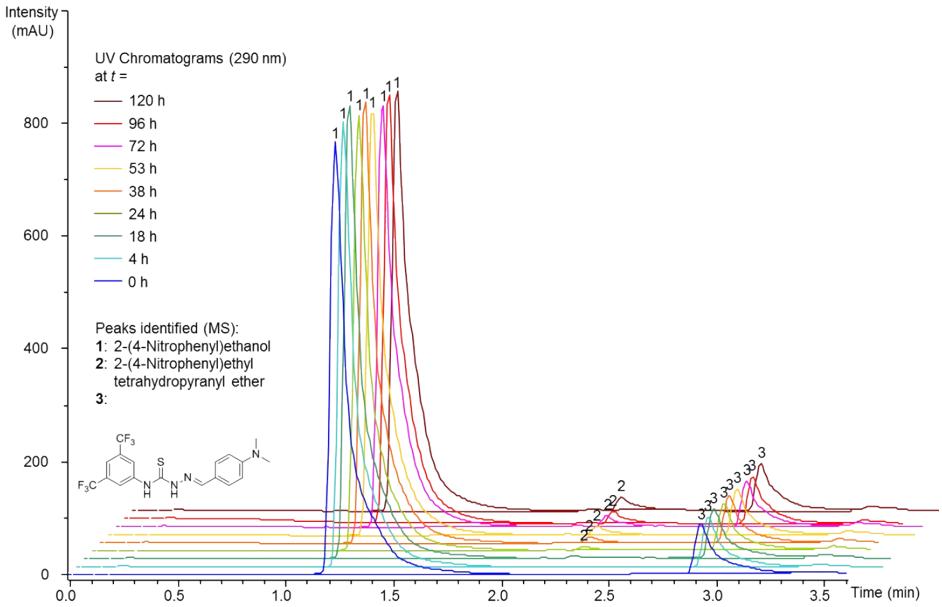

## Catalyst: 3

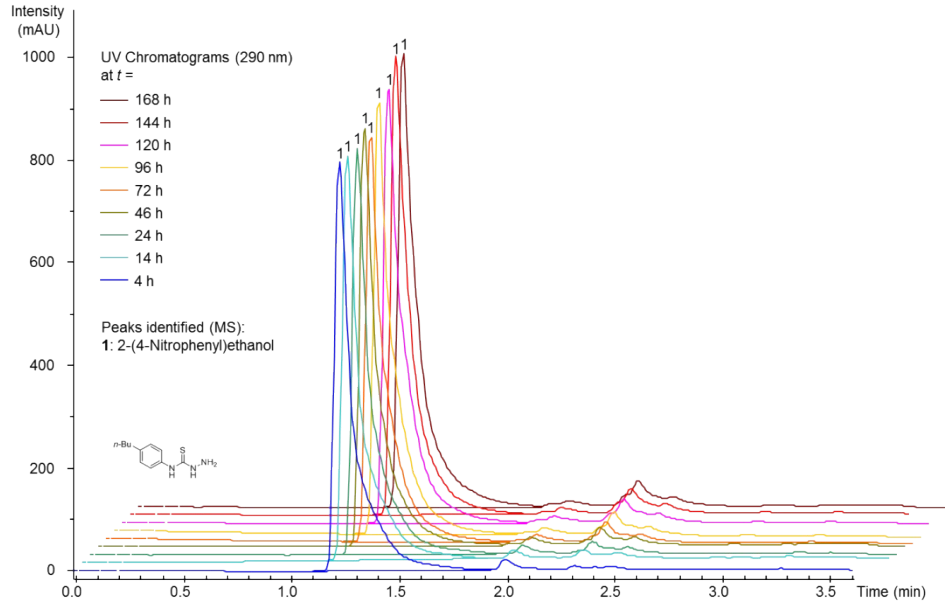


## Catalyst: 3a

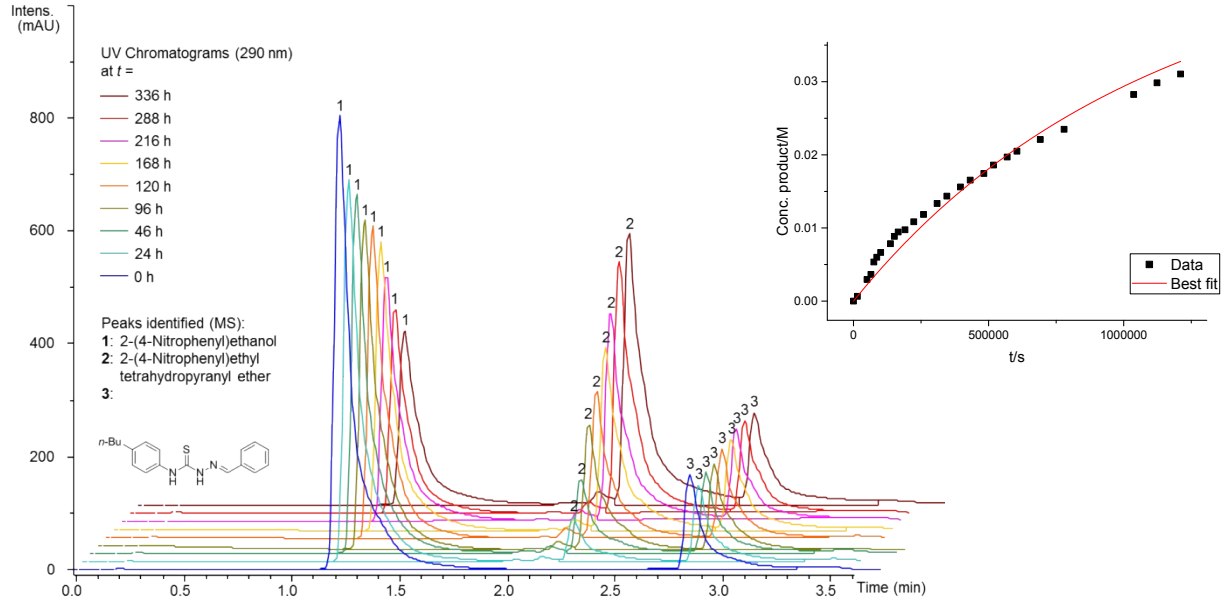

## Catalyst: 3b

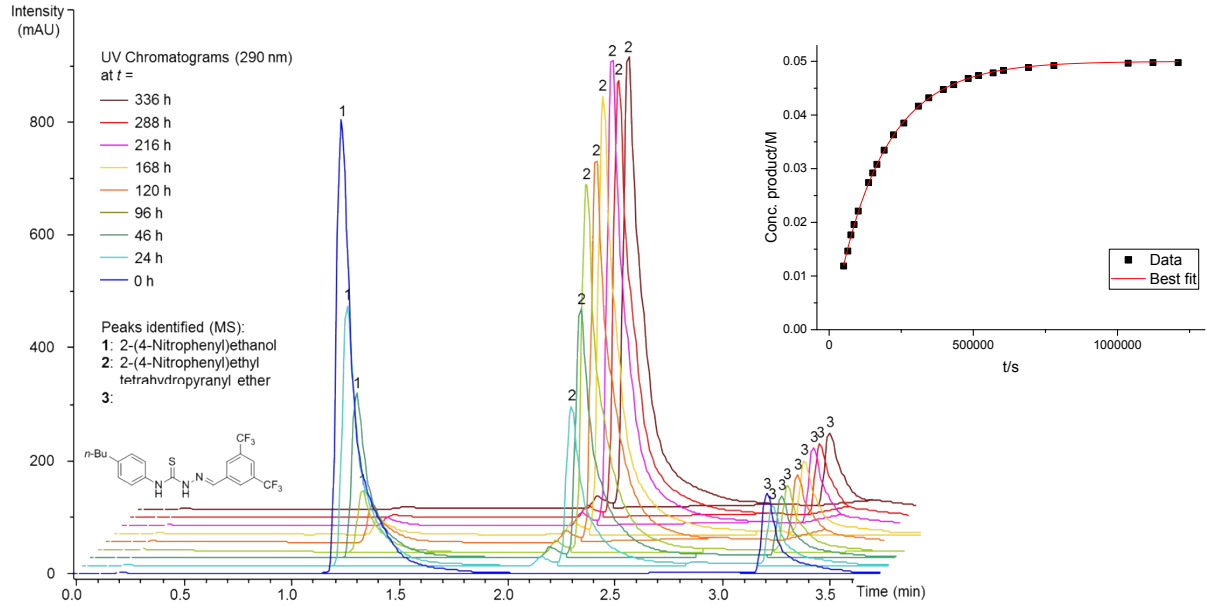


## Catalyst: 4

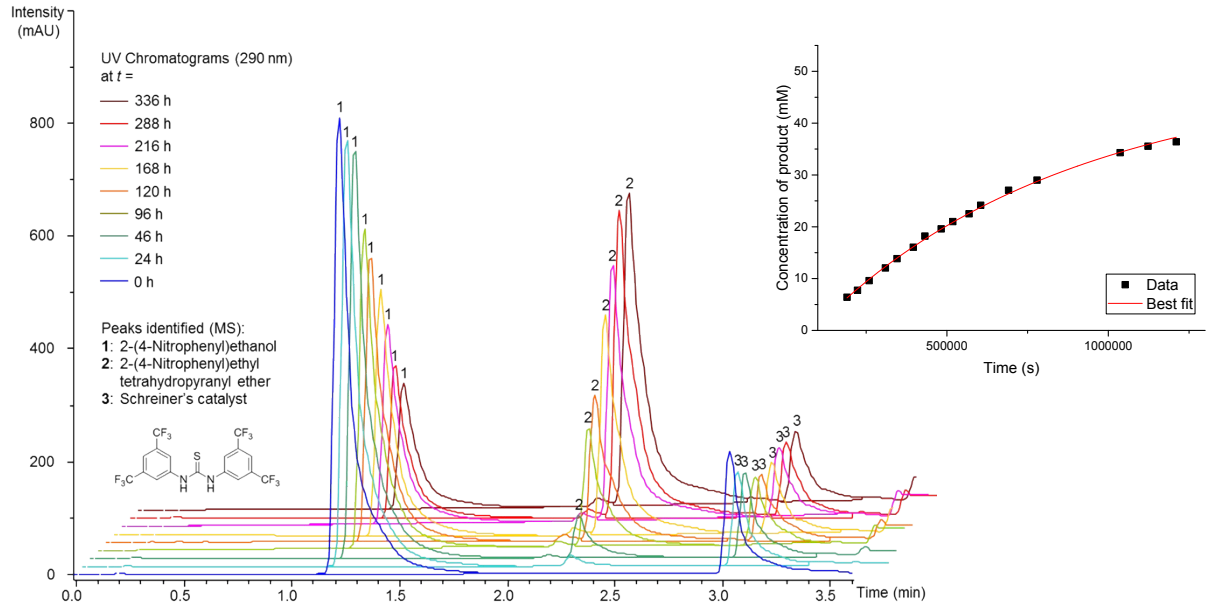

# 4. Supplementary mechanistic discussion

The non-acid-catalyzed tetrahydropyranylation can be considered a two-step process consisting of a proton transfer step and a C-O bond formation step. To evaluate which pathway (i.e. which order of the two steps) is the most likely, a two-dimensional reaction coordinate is illustrated below. In this diagram, the starting materials are in the bottom left corner, while the product is in the top right corner. Thus, starting from the bottom left, the mechanism leading to product is best described by the path requiring the least amount of energy that ends in the top right corner.

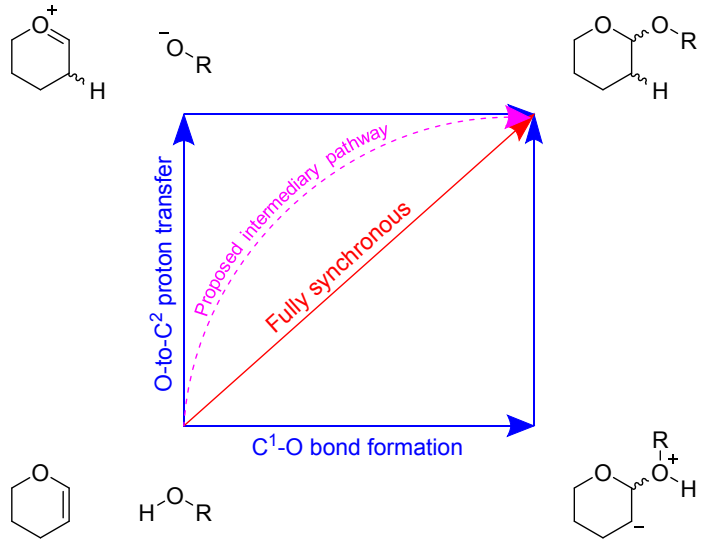


In one of the stepwise pathway, the proton transfer would occur before the C-O bond formation (first up, then right) and in the other stepwise possible pathway the C-O bond formation would occur before the proton transfer (first right, then up). Since formation of carbanions, even the stabilized one illustrated in the bottom right corner, requires strong bases, the stepwise pathway going via an oxonium ion/carbanion and then an intramolecular proton transfer (first right, then up) seems highly unlikely. On the other hand, the other stepwise pathway proceeds via a much more likely ion-pair consisting of an oxocarbenium ion and an alcoholate. Thus, the most likely stepwise mechanism must be the first-up-then-right pathway.

The red diagonal arrow illustrates the formally forbidden [2+2] cycloaddition pathway, in which the proton transfer and C-O bond formation steps are fully synchronous.

Note that the upwards direction represents increasing electron-density on the alcohol oxygen, while the rightwards direction represents loss of electron-density. The Hammett analysis of the phenol substrates (Figure 1 (manuscript), Table S4 (p. S21)) tells us that alcohol oxygen experiences loss of electron-density in the transition state. Thus, if the mechanism is stepwise, the rate-determining step must be the last step, the nucleophilic attack of the alcoholate on the oxocarbenium ion (moving to the right), rather than the first proton transfer step (moving upwards).

The dashed pink arrow symbolizes (roughly) the pathway followed in the mechanistic cycle proposed in Figure 4. The reasons for settling on this proposal will be discussed in the following sections.

## Summary of most important mechanistic evidence and discussion

The following is a list of findings about the mechanism under investigation. Below each finding, its main argument(s) are presented, and below that we present our interpretation of what each finding indicates about the mechanism.

- *The thiosemicarbazone catalyst is not working as a Brønsted acid catalyst*
    - The p$K_a$ of the best catalyst (11.5 in DMSO) was shown to be higher than the pKa of benzoic acid (11.1 in DMSO) (p. S44-S46).
        - This indicates that the catalyst works by forming a supramolecular complex.
- *The best catalysts are the most electron-deficient ones*
    - A positive slope was achieved in the Hammett plot made by using catalysts with different *p*-substituents (Figure 1 (manuscript), Table S4 (p. S21)).
        - This indicates that the catalyst interacts with an electron-rich species, i.e. the catalytic effect could be from the dual hydrogen-bonding motif in the thiosemicarbazone, akin to thiourea organocatalysis.
- *The catalysts show no interaction with DHP, but a small interaction with alcohols*
    - As evidenced by NMR titrations (Table S6 (p. S41)).
        - This indicates that the catalyst substrate complex must be between the catalyst and the alcohol, not between the catalyst and DHP.
- *During the transition state, the alcohol substrate (at least in the case of phenols) either builds up positive charge or loses negative charge*
    - Because of the negative slope in the Hammett plot made by using phenol substrates with different *p*-substituents (Figure 1 (manuscript), Table S4 (p. S21)).
        - This indicates a late transition state (in an electrocyclic type mechanism) or that the second step (phenolate nucleophile attack on DHP oxocarbenium ion) is rate-determining (in a stepwise mechanism).

The following energy diagram illustrates possible mechanistic pathways for the uncatalyzed reaction (red, not observed in practice), as well as two possible versions of the thiosemicarbazone-catalyzed reaction (blue and pink, will be explained below) as imagined based on the available data and mechanistic clues.

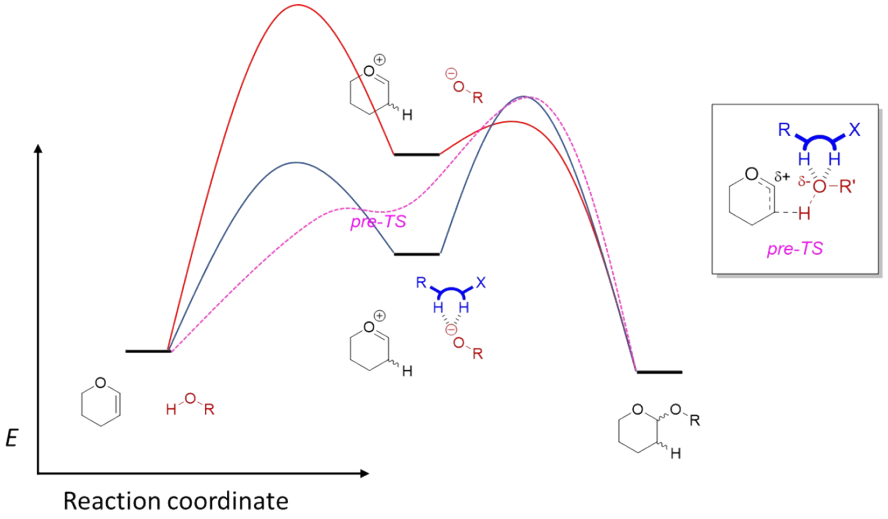

In the completely stepwise mechanism (blue) the stabilizing effect of the catalyst lowers the energy of the intermediate ion-pair by stabilizing the phenolate. This stabilization both lowers the energy-barrier for its formation, but also heightens slightly the barrier for the subsequent ion-pair collapse, which is in accordance with the Hammett plot-based observation that the second step must be rate-determining.

An intermediary pathway for the catalyzed reaction is also shown (pink dashed pathway). This pathway resembles the stepwise in the way that it starts by partial proton transfer to build up some degree of charges on the substrates, stabilized by the catalyst in a so-called pre-TS (inset), but instead of proceeding to form a fully charge-separated ion-pair, the C-O bond formation also starts to take place in a rate-determining electrocyclic transition to form the product (Figure 4 (manuscript)).

The available data does not allow a full distinction between a stepwise mechanism and a synchronous mechanism, but it does show that the rate-determining step in a possible stepwise mechanism would have to be the second step, i.e. the collapse of the phenolate/oxocarbenium ion-pair. Even with the stabilizing effect of the catalyst, however, it seems questionable that the first step, formation of two fully charged species in an apolar solvent (in which the reaction performs much better, see Table S1), requires less energy than the second step, the ion-pair collapse. This observation also suggests a mechanism in which full charge-separation is not achieved, i.e. an intermediary pathway.

Though the available data does not allow us to rule out a stepwise mechanism, Kotke and Schreiner's calculations on the thiourea-catalyzed version of this reaction (ref. 7b of the manuscript) showed a mechanism following a pathway intermediary between stepwise and synchronous. This pathway is approximated by the pink arrow in the two-dimensional reaction coordinate on the previous page. None of the data obtained in this study seems to contradict the mechanism put forward by Kotke and Schreiner, and therefore we propose that the thiosemicarbazone-catalyzed version of this reaction follows a similar mechanism (Figure 4 (manuscript)).

# 5. Double Hammett Analysis

A range of *para*-substituted phenols (Y in scheme 4.1) were reacted with **DHP** under catalysis by thiosemicarbazone **1c**. Similarly, a range of *para*-substituted thiosemicarbazones (X in scheme 4.1) were used to catalyse the tetrahydropyranylation of 4-methoxyphenol.

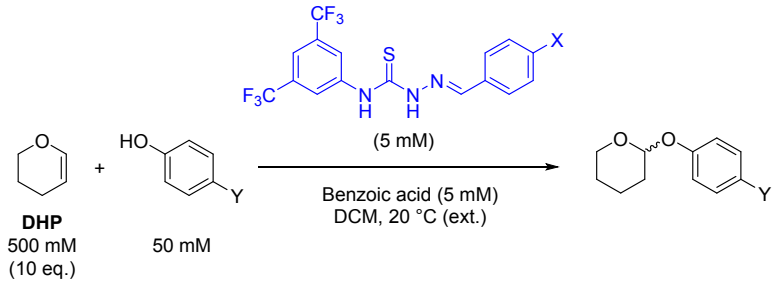


**Scheme 4.1:** Conditions employed for two-way Hammett plot investigation.

These experiments were carried out by preparing a range of solutions as described in the scheme above. Depending on the phenol, response factors between starting material and products were significantly different from 1, possibly due to the fact that the chromophore (the aromatic ring on the phenol starting material and aryl tetrahydropyranyl ether product) is now in direct conjugation with the reacting oxygen atom.

## Determination of response factors

The response factors are defined as the ratio between peak area of the starting material ($A_{s.m.}$) and the peak area of the product ($A_p$) at the given wavelength of the HPLC-UV experiment (Table S3 lists these wavelengths for each reaction). That is, the response factor is defined as $\frac{A_{s.m.}}{A_p}$. They can be calculated simply using the area underneath the peak for the starting material at t = 0 min, and the area underneath the peak of the product at full conversion. In some cases, the reactions were not followed all the way to full conversion. In these cases we found it possible to identify the response factors by plotting the sum of the peak areas for the starting material and the product as a function of conversion (in %), and iteratively change the response factor until a best linear fit was achieved (see graphs in lower left corner of pages S19-S24). This is possible under the assumption that starting material is only converted into product (which seems reasonable based on the lack of emergence of significant byproduct peaks in the chromatograms on pages S19-S24), which allows the use of Lambert-Beer's law to conclude that the change in total area as a function of conversion must be linear. Once the best linear fit has been found, $A_{s.m.}$ is found be calculating reading the values at 0 % respectively, since at 0 % conversion, the sum of the peak areas of starting material and product comes from starting material alone. Conversely, $A_p$ can be determined by reading the peak area sum at 100 % conversion, since it represents the area of the product peak only.

## Use of response factors when performing tetrahydropyranylation on phenol substrates

In our case, the response factors are only used when performing the tetrahydropyranylation with phenols. During the reaction, the phenol OH-group is changed to an O-alkyl group, and this alters the spectroscopic nature of the chromophore (the aromatic ring of the phenol). Thus, the absorptivity of the product cannot be assumed to be identical to the absorptivity of the starting material (at the same wavelength). A list of (local) $\lambda_{max}$ values for starting materials (ArOH) and products (ArOTHP) as well as the UV channel at which the reaction was followed and the corresponding response factor at this wavelength is seen in Table S3. In reactions with 2-(4-nitrophenyl)ethanol (i.e. not a phenol) as the substrate, the OH-group is not in conjugation with the chromophore, and as expected no significant change in total area was seen during the reaction in these cases (inset in Figure S2), and the maximum absorbance wavelength was unaltered (279 nm).

***Table S3: Absorption Maxima and Response Factors from Double Hammett Investigation***

| Y | $\lambda_{max}$ (ArOH) (nm) | $\lambda_{max}$ (ArOTHP) (nm) | UV Channel | Response factor |
|---|---|---|---|---|
| $NO_2$ | 316 | 307 | 290 nm | 0.78 |
| $CO_2Me$ | 256 | 253 | 255 nm | 1 |
| Br | 283 | 279 | 290 nm | 2.1 |
| H | 272 | 270 | 272 nm | 1.6 |
| Me | 280 | 277 | 290 nm | 4.1 |
| OMe | 290 | 286 | 290 nm | 1.3 |

Using these response factors, the concentration of product could be plotted as a function of time, and the second-order rate constants could be determined as described above (Table S4).

***Table S4: Second-Order Rate Constants Used for Double Hammett Analysis***

| # | X | Y | $k_2$ ($\cdot 10^{-5}$ $M^{-1}$ $s^{-1}$)[a] | # | X | Y | $k_2$ ($\cdot 10^{-5}$ $M^{-1}$ $s^{-1}$)[a] |
|---|---|---|---|---|---|---|---|
| 1 | $NO_2$ | $NO_2$ | 2.6 ± 0.7 | 7 | CN (**1i**) | OMe | 11.3 ± 0.7 |
| 2 | $NO_2$ | $CO_2Me$ | 5.76 ± 0.10 | 8 | $CF_3$ (**1j**) | OMe | 10.0 ± 0.3 |
| 3 | $NO_2$ | Br | 10.7 ± 0.9[b] | 9 | Br (**1k**) | OMe | 6.2 ± 0.3 |
| 4 | $NO_2$ | H | 13.18 ± 0.03 | 10 | H (**1a**) | OMe | 1.59 ± 0.11 |
| 5 | $NO_2$ | Me | 17.1 ± 1.5 | 11 | *t*-Bu (**1l**) | OMe | 0.71 ± 0.03 |
| 6 | $NO_2$ | OMe | 24 ± 2 | 12 | OMe (**1m**) | OMe | 0.716 ± 0.013 |

Conditions as per scheme 4.1. [a] Standard deviation based on duplicate measurements or better are given. [b] Standard error on fit.

## On substituent constants for Hammett plots

### Catalysts

The catalyst Hammett plot shows better linearity when plotted against $\sigma$ than when plotted against $\sigma^-$, as is illustrated by the two plots below:

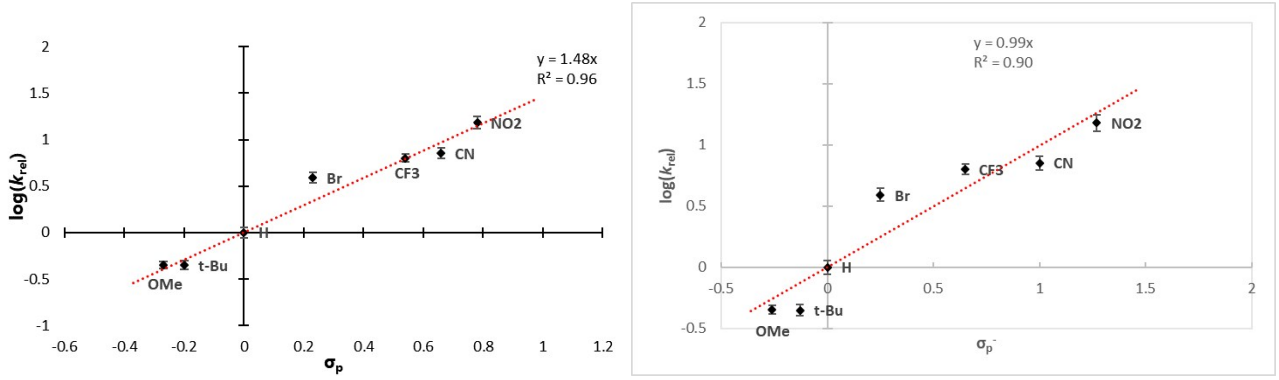


The $\sigma^-$ substituent constants where developed for aromatic systems where charges on the benzylic(-like) position (such as in phenolates or aniliniums) could be delocalized into substituents with high degree of mesomeric effects (such as $NO_2$ or carbonyl groups).[2] If the thiosemicarbazones in this study functions in a manner similar to thioureas (as is the theory), no build-up of charges on the benzylic position is expected, and therefore it comes as no surprise that the $\sigma^-$ values leads to a plot of lower linearity.

The sign and magnitude of the slope (+1.48) indicates that the catalyst experiences a build-up of electron-density during the reaction, and that the reaction is more sensitive to substituent effects than the ionization of benzoic acid (the reaction for which the Hammett plot slope is defined as 1.00).

## Phenol substrates

For the phenol substrates, the $\sigma^-$ substituent constants should produce the most linear slope, as they were developed for use with phenols in mind, among others. In this case, both $\sigma^-$ and $\sigma$, however, produce reasonably good linear fits, as shown in the plots below:

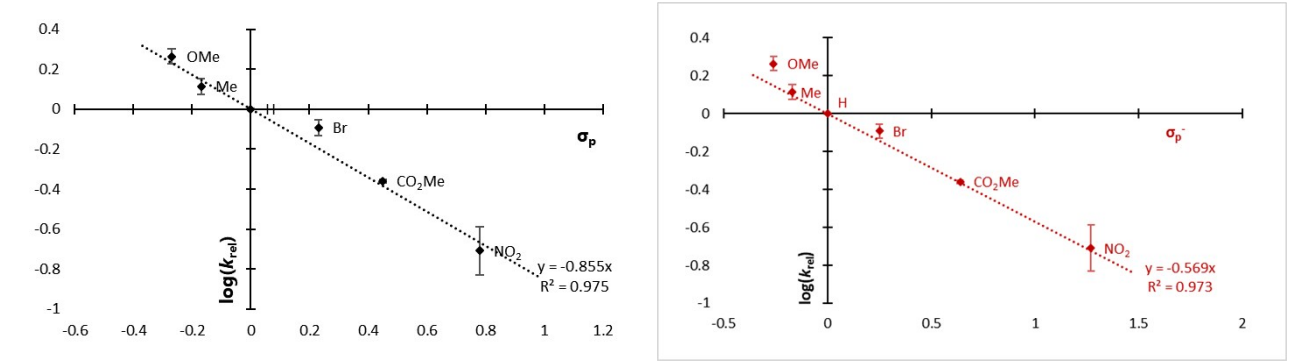


The observed rate for 4-methoxyphenol (marked 'OMe') seems to be higher than expected based on use of either set of substituent constants, and that, along with the relatively large error for 4-nitrophenol (marked '$NO_2$'), somewhat explains the good fit obtained with the $\sigma$ values. Omitting the 4-methoxyphenol data point (shown in blue below) from the linear plot results in a fit with excellent linearity, as shown below:

[2] L. P. Hammett, *J. Am. Chem. Soc.*, 1937, **59**, 96.

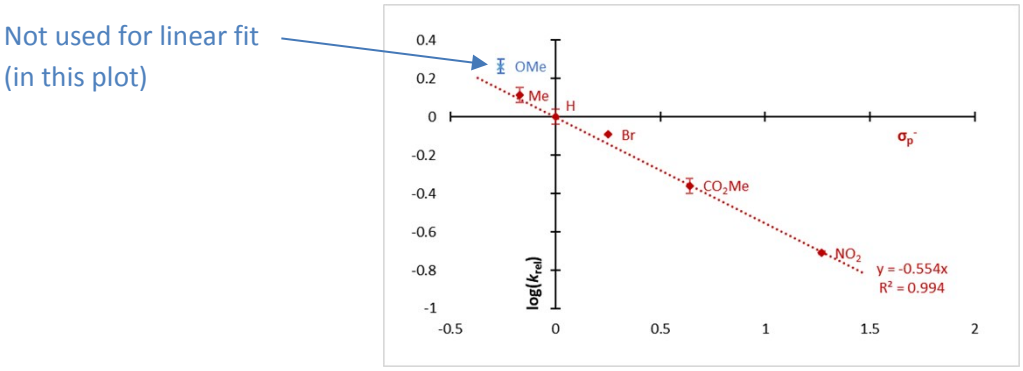


The negative sign of the slope (-0.57) indicates a loss of electron-density on the phenol during the reaction.

The slope in this reaction has a lower magnitude than typical reactions of phenolates, where the phenol substrate experiences loss of a full formal charge during the reaction. For example, the reaction of substituted phenolate ions with ethylene oxide gives a Hammett plot with a slope of -0.95, while the alkylation of substituted phenolate ions with ethyl iodide results in a slope of -0.99.[8] That the tetrahydropyranylation under scrutiny here has a slope of lower magnitude could be a sign that the rate-determining step does not include loss of a full formal charge, corresponding to a mechanism in which the phenol is not fully deprotonated, or that a fully deprotonated phenol, if formed, is stabilised (e.g. by dual hydrogen bond-donation from the thiosemicarbazone catalyst). However, it could also simply be because this reaction shows lower inherent sensitivity on the substituents than the two phenolate examples just mentioned.

**Representative UV Chromatograms and Time-Dependent Concentration Changes from Double Hammett Analysis of a Range of Phenols and Catalyst 1c and 4-Nitrophenol**

**Catalyst 1c and 4-nitrophenol:**

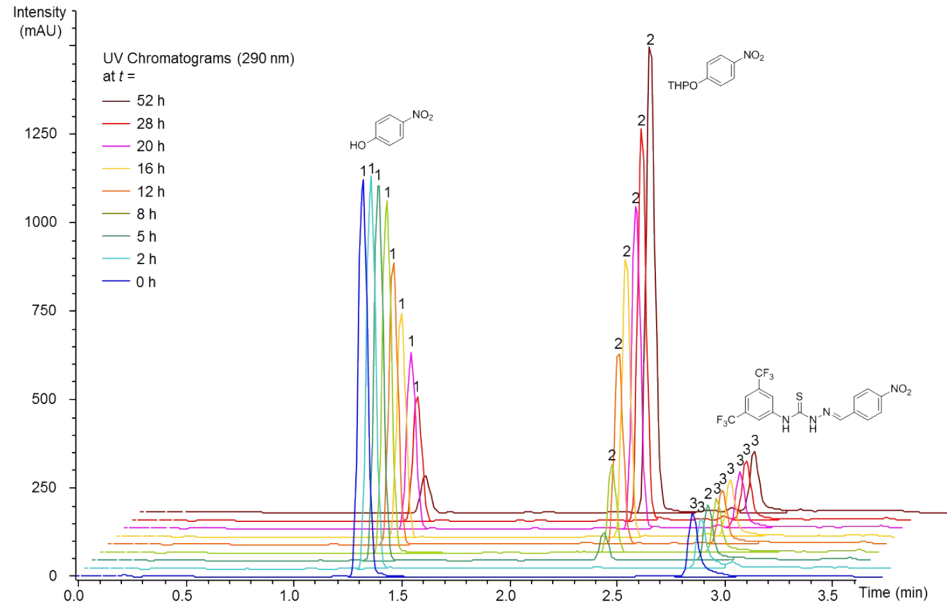


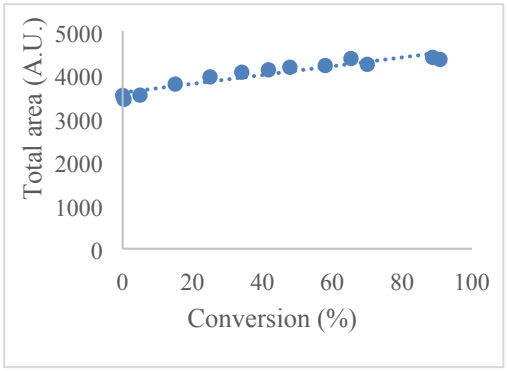


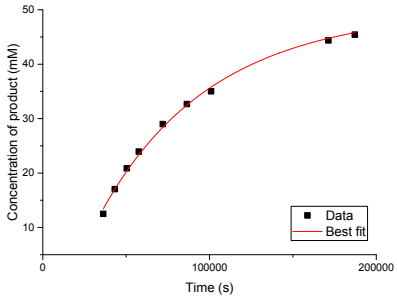

## Catalyst 1c and 4-methoxycarbonylphenol

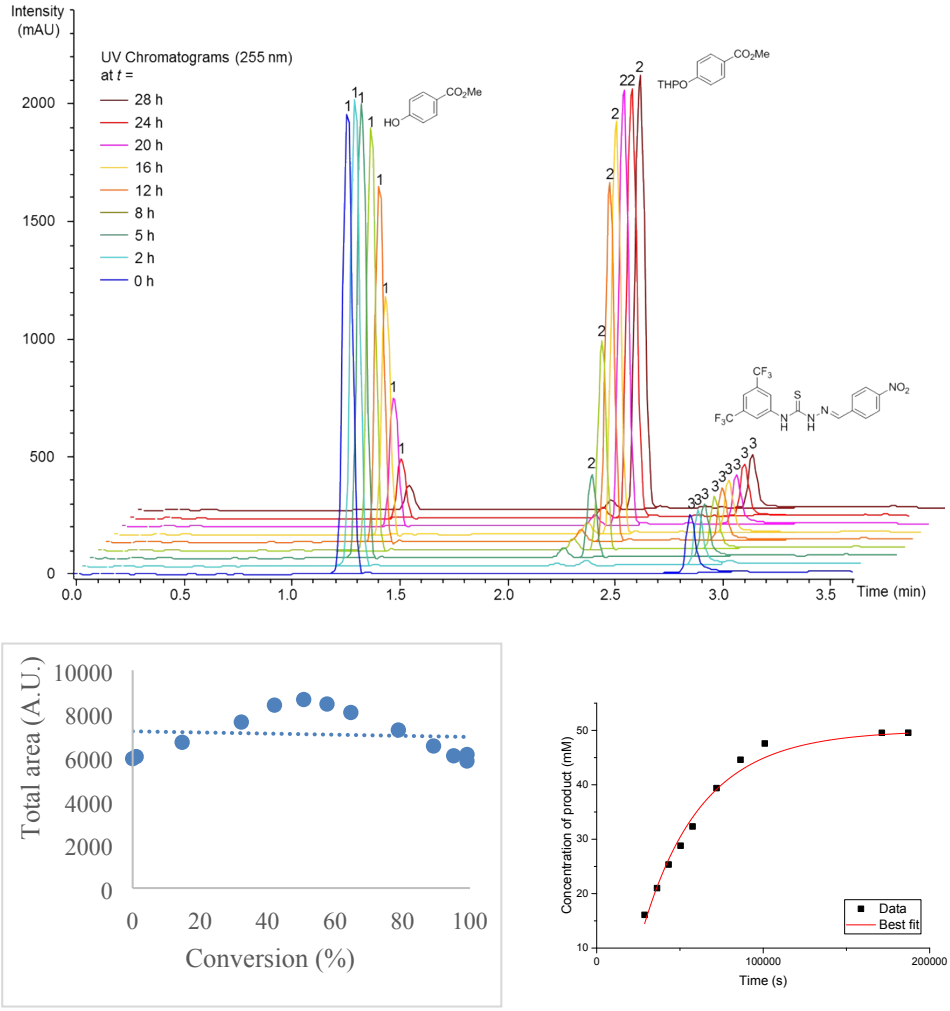


**Note:** This specific reaction exhibited a non-linear response in the total area vs. conversion graph, suggesting that a side-reaction takes place. However, the HPLC chromatograms (UV at 255 nm) suggests no significant formation of byproducts and no precipitation was detected in the vial during or after the reaction. Due to the peculiar nature of this total area vs. conversion curve, the response factor was set to 1.

## Catalyst 1c and 4-bromophenol

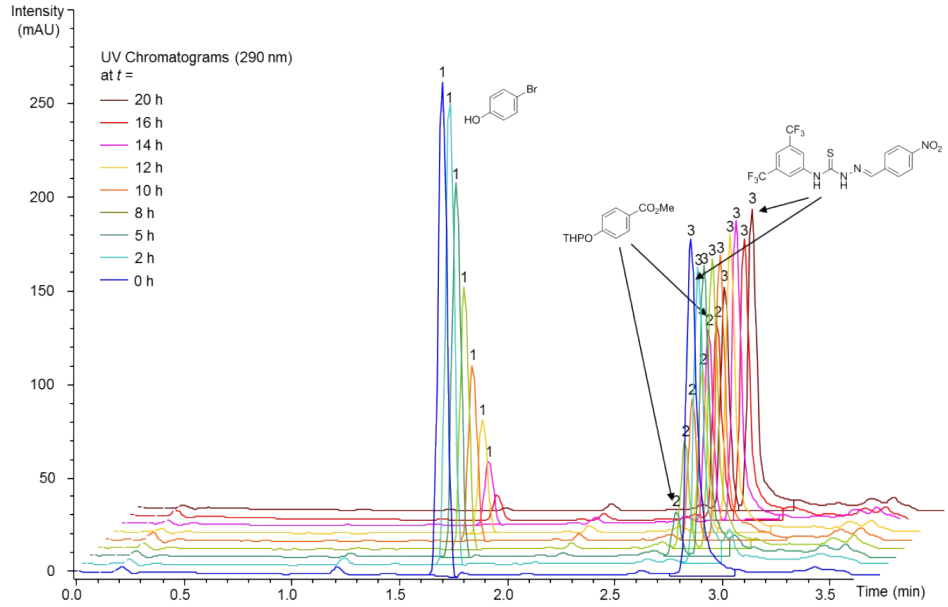


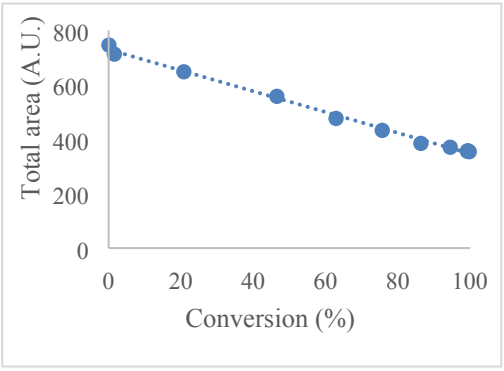


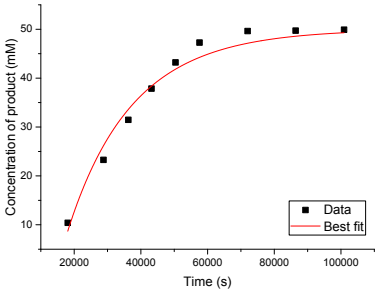

## Catalyst 1c and phenol

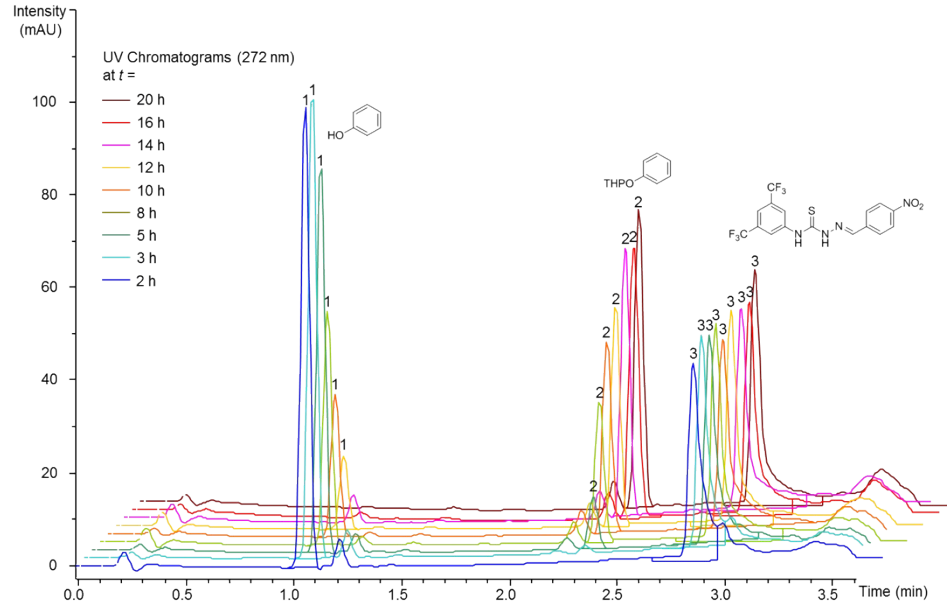


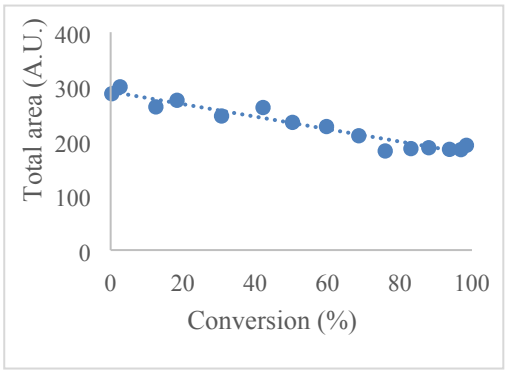


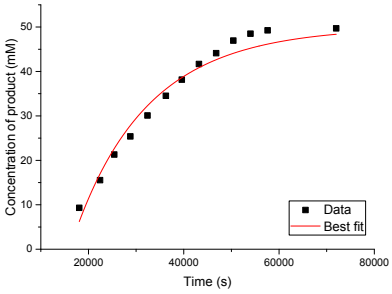

## Catalyst 1c and 4-methylphenol

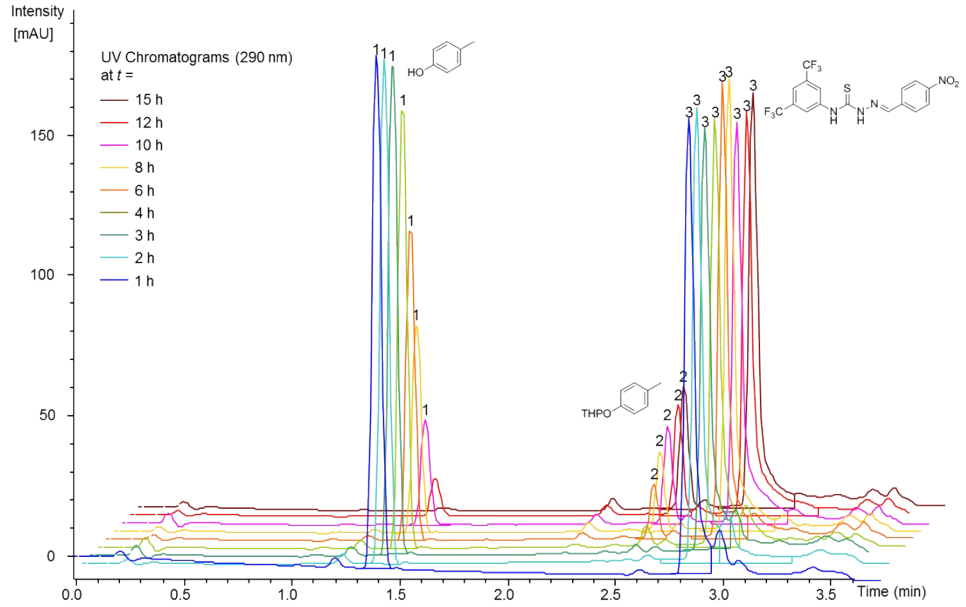


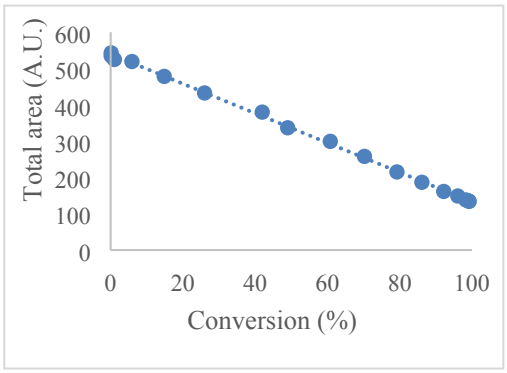


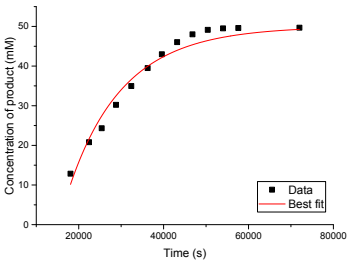

## Catalyst 1c and 4-methoxyphenol

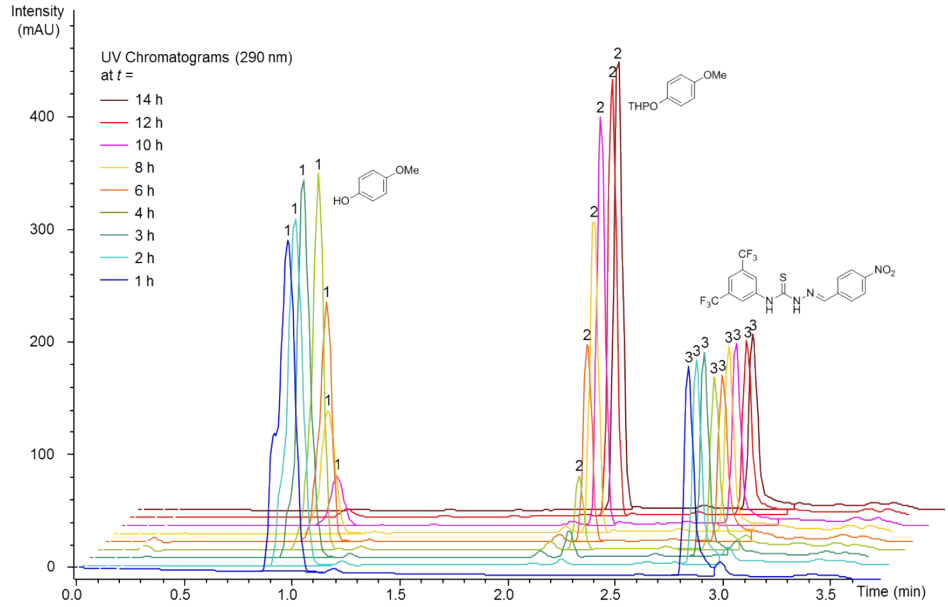


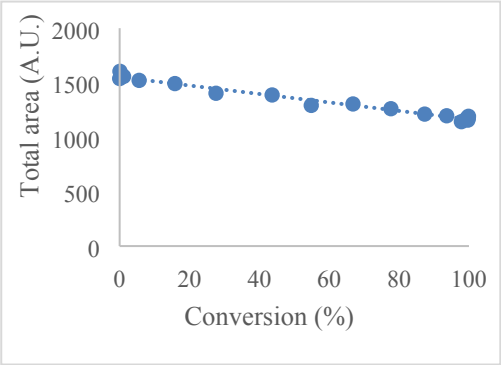


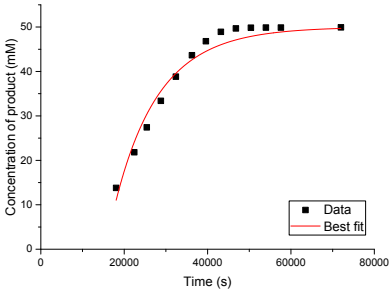

# 6. Investigations on the Order of the Reactants

A range of experiments were conducted in order to elucidate the order of the reactants and the dependency on concentration of catalyst.

### First-order Dependence on Alcohol Concentration

Firstly, the starting concentrations of **DHP**, benzoic acid and catalyst (**1c**) were kept constant while the starting concentration of the alcohol substrate (4-methoxyphenol) was varied (scheme 5.1).

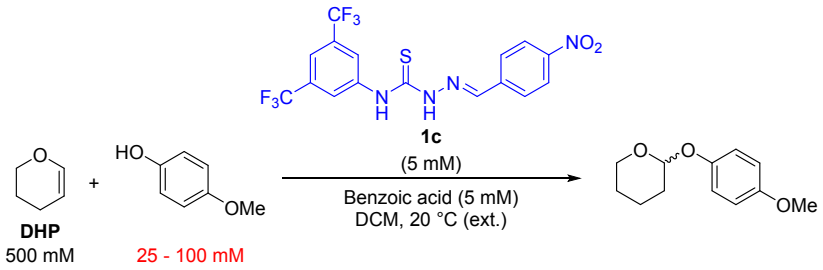


**Scheme 5.1:** Conditions applied to evaluate the dependence on alcohol concentration.

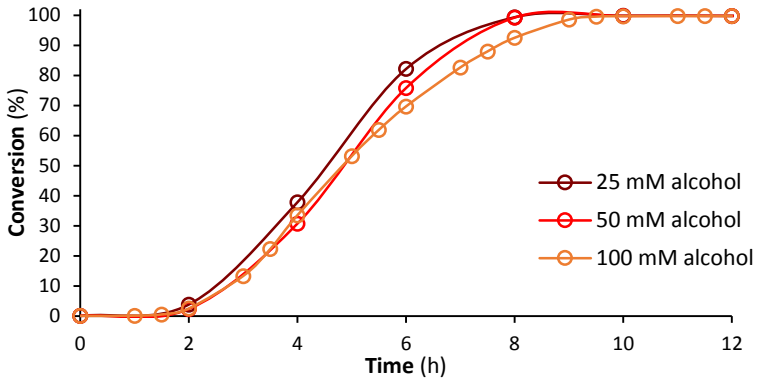


**Figure S 4:** Conversion profiles with three different starting concentrations of 4-methoxyphenol. No significant differences in conversion time were observed, indicating that the reaction rate is first-order dependent on alcohol concentration.

As is evident from figure s **4**, altering the alcohol starting concentration does not influence the overall reaction time. Thus, approx. 8 hours is needed to convert all of the alcohol under these conditions, no matter if the starting concentration of 4-methoxyphenol was 25, 50 or 100 mM.

Therefore, the turnover rate (in mol/s) must be roughly twice as fast with a starting concentration of 100 mM compared to a starting concentration of 50 mM. Likewise, the turnover rate (in mol/s) must be roughly half as fast with a starting concentration of 25 mM compared to a starting concentration of 50 mM. This supports the notion that the reaction rate is first-order with respect to the alcohol.

### First-order Dependence on DHP Concentration

Secondly, the starting concentrations of the alcohol (4-methoxyphenol), benzoic acid and catalyst (**1c**) were kept constant while the starting concentration of **DHP** was varied (scheme 5.2).

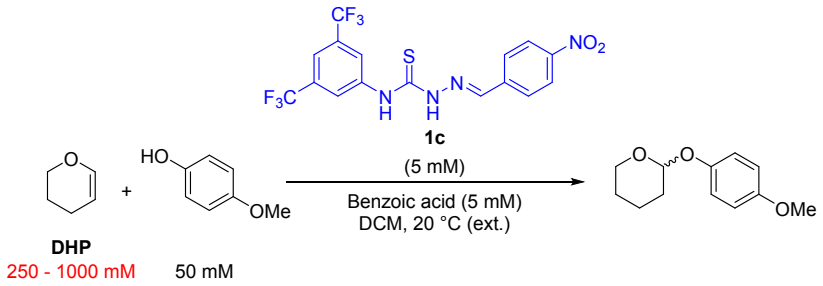


**Scheme 5.2:** Conditions applied to evaluate the dependence on **DHP** concentration.

As is evident from figure s **5**, changing the concentration of **DHP** dramatically influences the turnover rate of the alcohol, which is the species monitored during the reaction. Therefore, to assess the dependence on **DHP** concentration, the rate constant, $k_2$, was determined for each case.

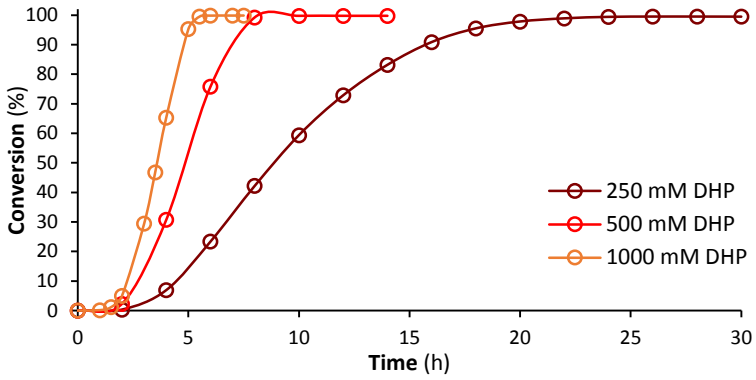


**Figure S 5:** Conversion profiles with three different starting concentrations of DHP.

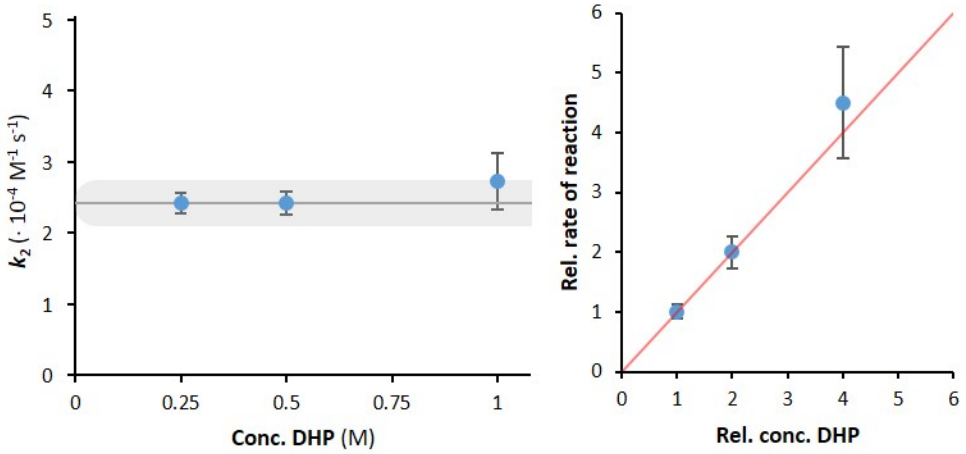


**Figure S 6: Left:** Rate constants (with error on fit from one measurement) determined at different concentrations of **DHP**. The grey line and surrounding grey area symbolise the mean value of $k_2$ and the standard deviation as identified from earlier experiments. **Right:** The relative rates of reaction are all, within error, on a straight line with a slope of 1 (red) when plotted against the relative concentration of **DHP**.

The rate constants were all identical to the previously determined value, within error (see figure s **6**, left). The relative rate of reaction, $r_{rel}$, (with the rate, $r$, determined as $[DHP]_0 \cdot k_2$) was plotted against the relative

starting concentration of **DHP** (figure s **6**, right). Since all the relative rates are, within error, on a straight line with a slope of 1, the reaction rate is first-order-dependent on the concentration of **DHP**.

### Addition of Benzoic Acid Increases the Reaction Rate

The starting concentrations of **DHP**, alcohol (4-methoxyphenol) and catalyst (**1c**) were kept constant while a set of reactions with varying concentrations of benzoic acid was monitored (scheme 5.3). The rate of the reaction at 0 mM benzoic acid concentration was estimated based on previous experiments with catalyst **1b** with and without benzoic acid.

As is evident from Figure S 7, higher concentrations of benzoic acid do promote slightly faster turnover and shorter induction times, though the rate at 10 mM benzoic acid concentration is not higher than at 5.0 mM concentration. This hints at a cooperative interaction between catalyst and benzoic acid, and prompted the use of benzoic acid in equimolar amounts to the thiosemicarbazone catalysts.

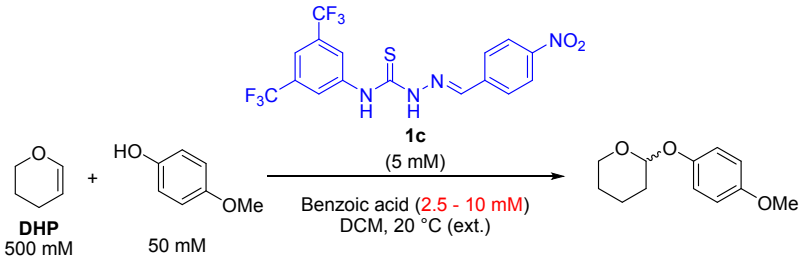


**Scheme 5.3:** Conditions applied to evaluate the importance of benzoic acid concentration.

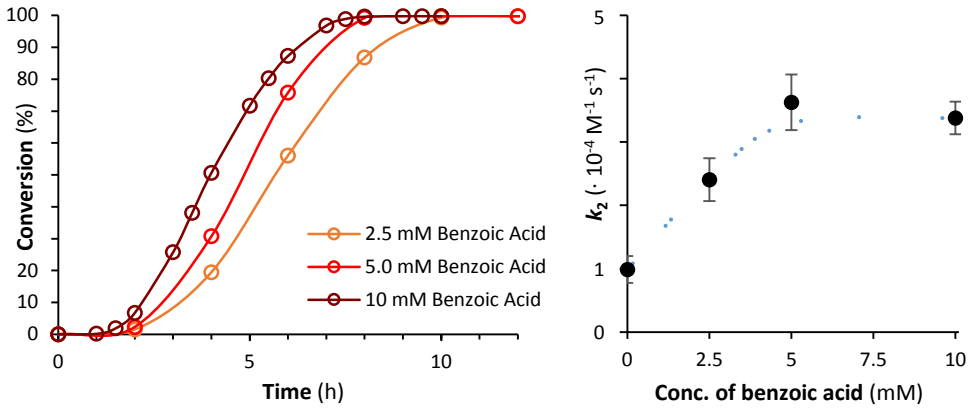


**Figure S 7: Left:** Conversion profiles with three different starting concentration of benzoic acid. **Right:** Second-order rate constants as a function of benzoic acid concentration. Data represented by black dots. Error bars are based on triplicate measurements or better. The blue dotted line is merely to guide the eye.

### Reaction Rate Decreases with Lower Catalyst Loading

Thirdly, the starting concentrations of **DHP**, alcohol (4-methoxyphenol) and benzoic acid were kept constant while the concentration of catalyst (**1c**) was lowered (scheme 5.4).

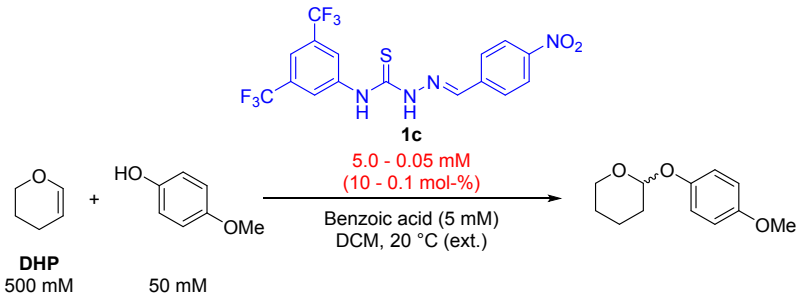


**Scheme 5.4:** Conditions applied to evaluate importance of catalyst loading.

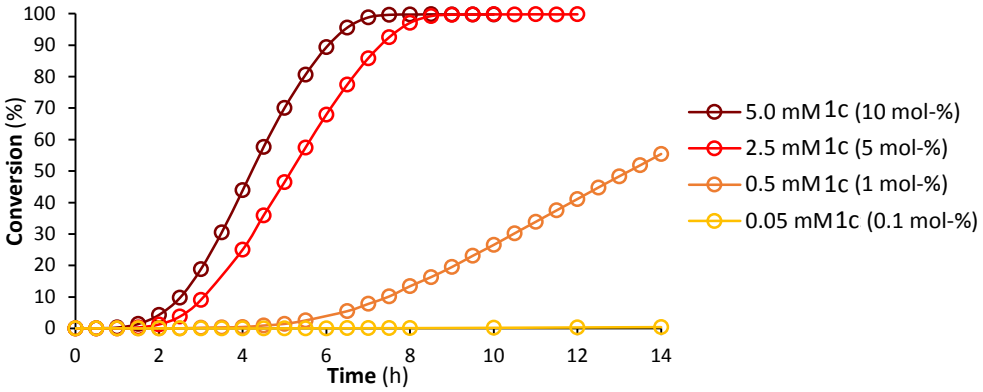


**Figure S 8:** Conversion profiles for four different catalyst loadings.

As is evident from Figure S 8, the reaction rate is only slightly reduced when 5 mol-% catalyst is used instead of 10 mol-%. However, lowering the catalyst loading to 1 mol-% significantly reduces reaction rate, and the catalytic capability appears to wither away with even lower catalyst loadings.

## The Reaction Is Not Autocatalytic in Tetrahydropyranyl Ether

To investigate if the observed induction period was caused by the reaction being autocatalytic (e.g. that the presence of tetrahydropyranyl ether product promotes its own production), an experiment in which product was added to the reaction mixture before addition of alcohol was performed (scheme 5.5).

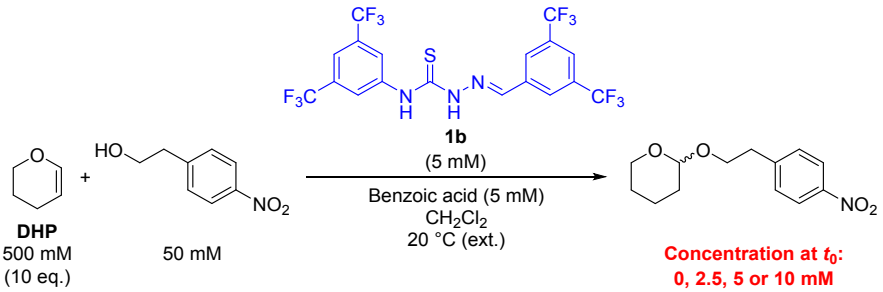


**Scheme 5.5:** Reaction conditions employed to check for autocatalysis. The reaction was performed with and without several amounts of tetrahydropyranyl ether product present from the onset of the reaction.

If the reaction showed autocatalytic behaviour, the induction period should disappear (or at the least diminish considerably) in the reactions where product was present at the beginning.

However, as is seen in Figure S 9, the induction period remained the same, whether or not tetrahydropyranyl ether product was present from the beginning. The subsequent reaction slope showed no significant difference in reaction rate either, so it was concluded that autocatalysis was not the root of the induction period.

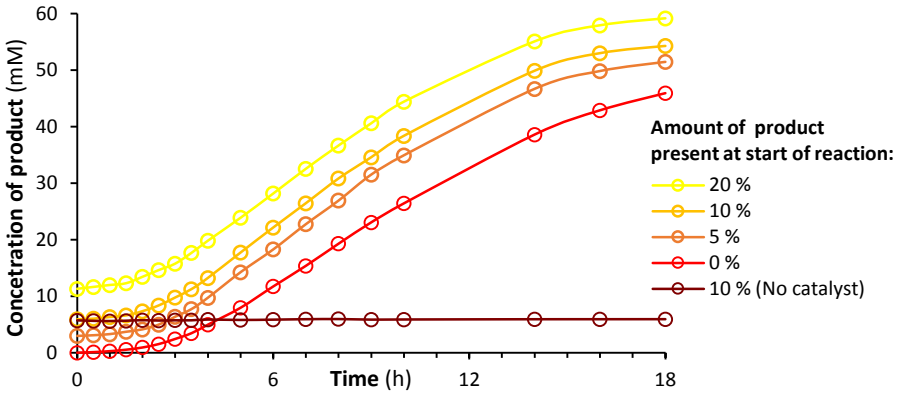


**Figure S 9:** Whether or not any tetrahydropyranyl ether was present at the starting time of the reaction had no influence on the rate of reaction or the induction period

# 7. NMR Titrations

To investigate how thiosemicarbazone catalysts interact with the remaining species in the solution, a range of NMR titrations were performed to determine binding constants between thiosemicarbazone catalyst **1c** and DHP or 4-methoxyphenol.

The following pages show representative data for the dimerization and guest binding studies performed with the thiosemicarbazones of this study. All the dimerisation and binding studies were performed in $CDCl_3$ (treated with basic aluminium oxide before use) at 20 °C. Protons are dubbed $H^a$, $H^b$, and $H^c$ as per the structure below.

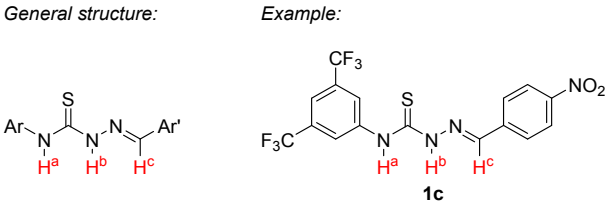


$H^c$ was assigned in catalyst **1b** and **1c** by HSQC by it being the only $^1H$ NMR singlet corresponding to one H (as evaluated by the integral) that has an HSQC cross-coupling to a $^{13}C$ NMR signal that does not split because of coupling to $^{19}F$ (green mark-up below). The only other $^1H$ NMR singlet corresponding to only one H (the *para*-H of the 3,5-bis(trifluoromethyl)phenyl) has an HSQC cross-coupling to a $^{13}C$ signal that does in deed split into what would be a heptet at slightly higher resolution because of coupling to the six magnetically equivalent fluorine atoms of the $CF_3$ groups (blue mark-up and inset):

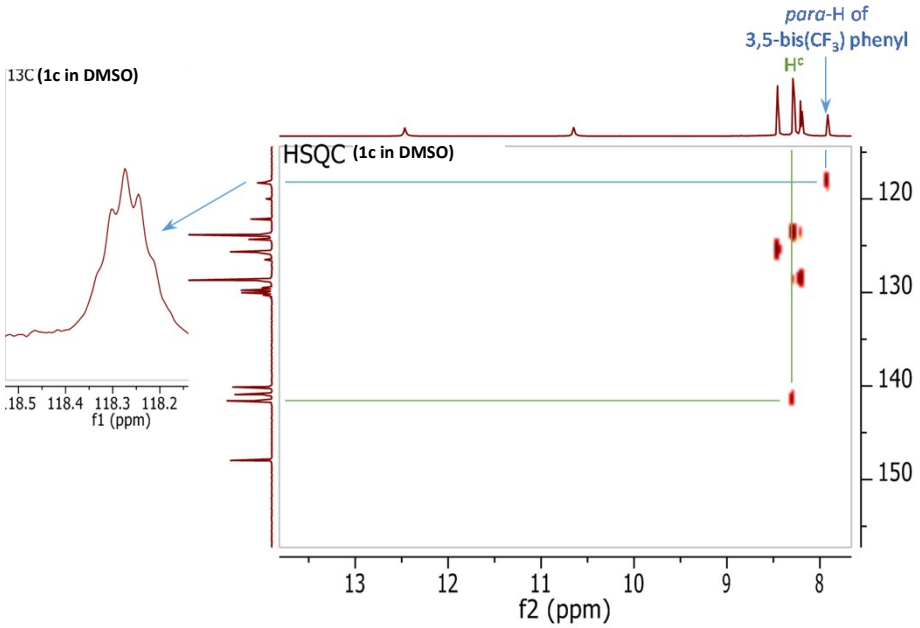


$H^a$ and $H^b$ are easily recognized by their characteristic broad $^1H$ NMR singlet signals above 10 ppm, as well as by their lack of cross-couplings in the $^1H$-$^{13}C$ HSQC experiment. $H^a$ was identified by a long-range coupling ($^3J$) to the *ortho*-carbons of the 3,5-bis(trifluoromethyl)phenyl as observed in an HMBC experiment:

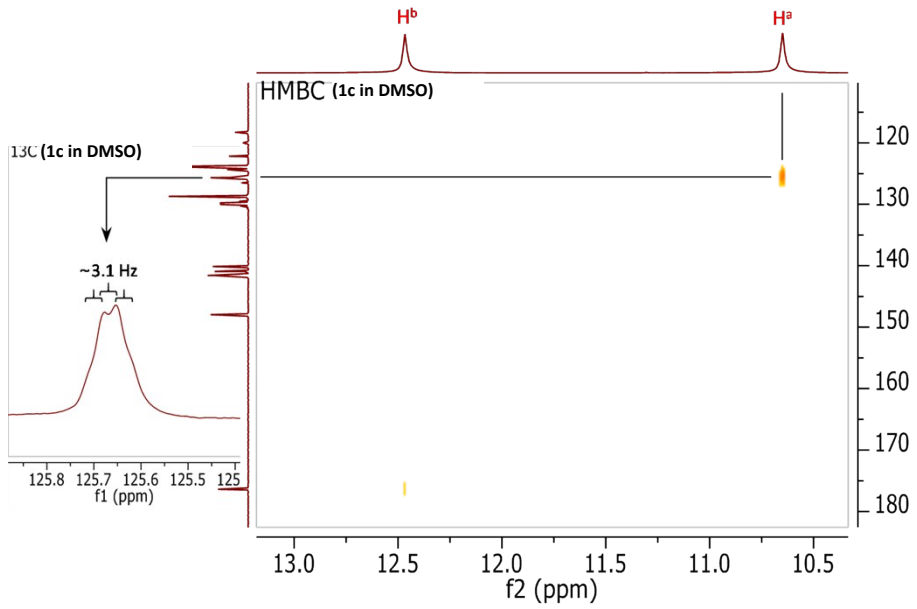


The $^{13}C$ signal from the *ortho*-carbons is easily recognized by its characteristic $^{3}J_{C\text{-}F}$ coupling, resulting in a quartet with a coupling constant of ca. 3.1 Hz (inset in figure above).[3]

$H^b$ was assigned by elimination, in that it must be the other NH-signal. Thus, the $H^b$ $^1H$ NMR signal was deemed the signal at highest ppm-value at high concentration of the catalyst. This signal was found to have a weak HMBC cross-coupling to the thiocarbonyl-C, but otherwise no other long-range couplings were seen.

Catalyst **1b** was assigned in the same manor, also using $^1H$-$^{13}C$ HSQC and $^1H$-$^{13}C$ HMBC in combination with ordinary NMR experiments. Assignments of catalyst **1b** was performed in $CDCl_3$. Due to low solubility in $CDCl_3$, the assignments for catalyst **1c** was performed in DMSO-$d_6$, and it was assumed that no significant change in signal position occurred when switching to $CDCl_3$. Catalyst **1b** and **1c** behaved in identical fashions with respect to magnitude and direction of chemical shift changes upon dilution in $CDCl_3$, which supports that the assignments of **1c**-signals in DMSO-$d_6$ are transferrable to $CDCl_3$.

$H^a$, $H^b$, and $H^c$ in catalysts other than **1b** and **1c** were assigned by inference, assuming $H^b$-signals to be more downfield than $H^a$-signals at high concentrations. $H^c$ was easily distinguished from the *para*-H of the 3,5-bis(trifluoromethyl)phenyl in that it had a much higher change in chemical shift during dilution, as is also evidenced by the dimerisation studies shown below.

[3] R. A. Newmark and J. R. Hill, *Org. Magn. Resonance*, 1977, **9**, 589.

## Dimerization Studies

Upon dilution of $CDCl_3$ solutions of several of the catalysts (**1a-c** and **3a-b**) it was found that all of the signals in their $^1H$ NMR spectra moved, and especially the two NH signals (dubbed $H^a$ and $H^b$) and the imine-CH ($H^c$) signal shifted significantly (Figure S 10). This is a strong indication that the molecules form supramolecular aggregates in solution.

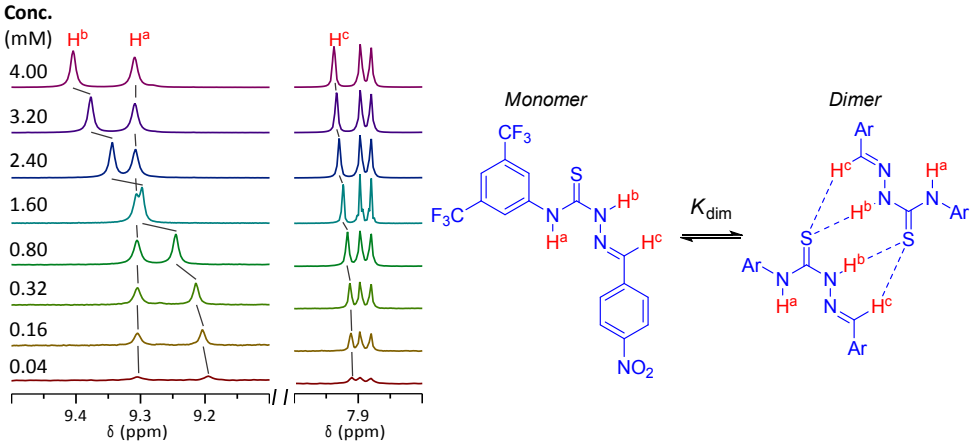


**Figure S 10:** Illustration of $^1H$ NMR signal shift upon dilution. This example is with catalyst **1c** in $CDCl_3$ at 20 °C. The direction and magnitude of the shifts are consistent with formation of a hydrogen-bonded dimer. The signal intensities are not to scale.

The magnitude and direction of the changes in the shifts indicate that the catalysts form hydrogen-bonded dimers in solution. The structure of the dimer seen above corresponds to the dimerization seen in the crystal structures (see below). In order to determine binding constants between the catalysts and any other molecules, it is necessary to determine the dimerization constant so as to be able to take it into account if needed.

A range of dilution experiments were performed and the chemical shift of $H^b$ was fitted to the following equation (fitted parameters in blue):

$$\delta_{obs} = \delta_m + (\delta_d - \delta_m)\frac{\sqrt{1 + 8K_{dim}[Catalyst]_0} - 1}{\sqrt{1 + 8K_{dim}[Catalyst]_0} + 1}$$

where $\delta_m$ and $\delta_d$ represent the "true" chemical shifts of the monomer and the dimer, respectively. $K_{dim}$ is the dimerization constant.[4]

Due to the large shift in all of the catalysts of the $H^b$ signal (Figure S 10), this signal was used to determine $K_{dim}$, though similar values, albeit with higher errors, were obtained upon fitting to the shift of other proton signals. The obtained dimerization constants are listed in Table S5.

[4] J. S. Chen and B. R. Shirts, *J. Phys. Chem.*, 1985, **89**, 1643.

***Table S5: Dimerisation Constants***

| | $K_{dim}$ ($M^{-1}$)[a] | | |
|---|---|---|---|
| **Catalyst** | Proton a[b] | Proton b[b] | Proton c[b] |
| **1a** | 12 ± 2 | 11.7 ± 1.0 | 12.8 ± 0.9 |
| **1b** | *c.n.d.* | 20.8 ± 1.0 | 21.5 ± 1.8 |
| **1c**[c] | *c.n.d.* | 39 ± 6[d] | 37 ± 5[d] |
| **3a** | 7.7 ± 0.5 | 12.3 ± 0.2 | 13.0 ± 0.2 |
| **3b** | 18 ± 2 | 43.3 ± 0.9 | 45.8 ± 1.3 |

Measured in $CDCl_3$ at 20 °C. [a] As obtained from fit to the changes in chemical shift of the proton indicated upon dilution. Errors given are standard errors on best fit. [b] Protons are named according to Figure S 10. [c] A value of (44 ± 6) $M^{-1}$ was obtained upon fit to the chemical shift of the *ortho*-H of the 3,5-bis(trifluoromethyl)phenyl. [d] Low solubility of catalyst **1c** in $CDCl_3$ at 20 °C gives high standard error on best fit. *c.n.d.*: Could not be determined.

Catalysts **1c** and **3b** show the highest propensity for dimerisation, though all of the catalysts show relatively low dimerization constants. Thus, at concentrations below 2 mM of catalyst **1c** less than 5 % of the catalyst molecules will be bound as dimers at any given time (assuming a $K_{dim}$ of 45 $M^{-1}$).

Based on this, it was determined that binding constants between catalysts and other molecules could be determined with reasonable accuracy without taking the effects of dimerization into account, as long as the catalyst concentration was kept below 2 mM. At these low concentrations, the catalysts exist primarily in the free monomer form, and thus would be free to form hydrogen bonds to other molecules.

Below are relevant parts of the $^1$H NMR spectra from the dilution experiments with catalysts **1a-c** and **3a-b**, along with best fit to the equation mentioned above.

### *Catalyst 1a*

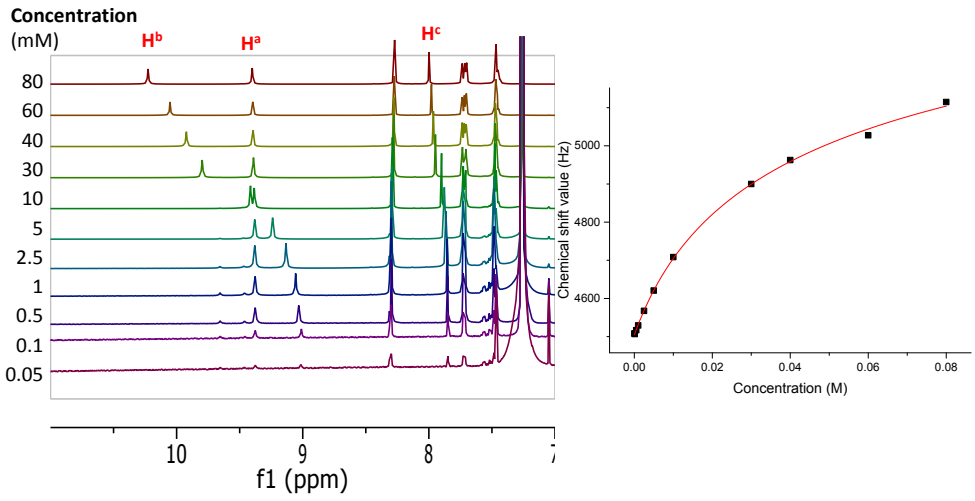

## *Catalyst 1b*

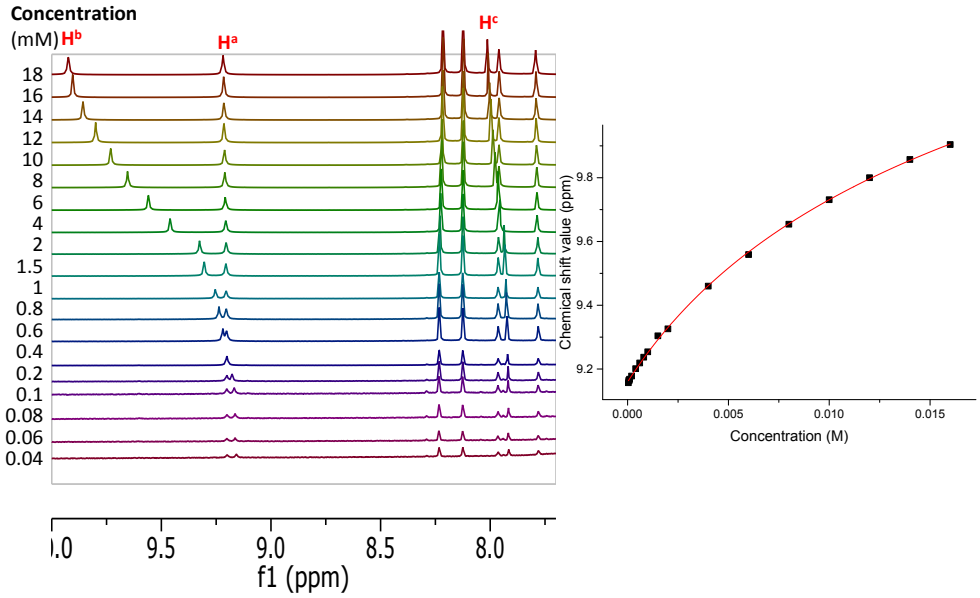


## *Catalyst 1c*

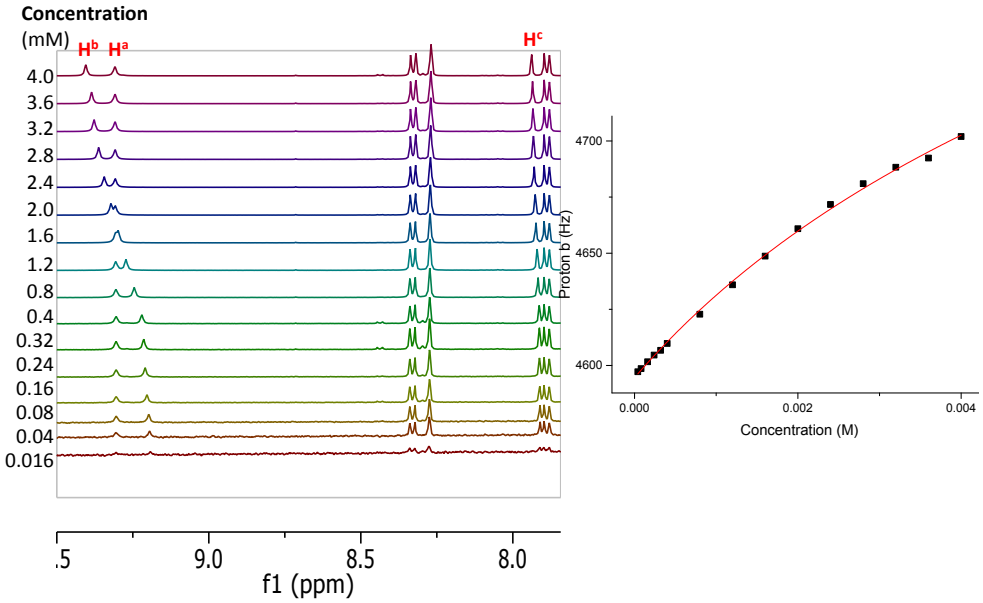

## *Catalyst 3a*

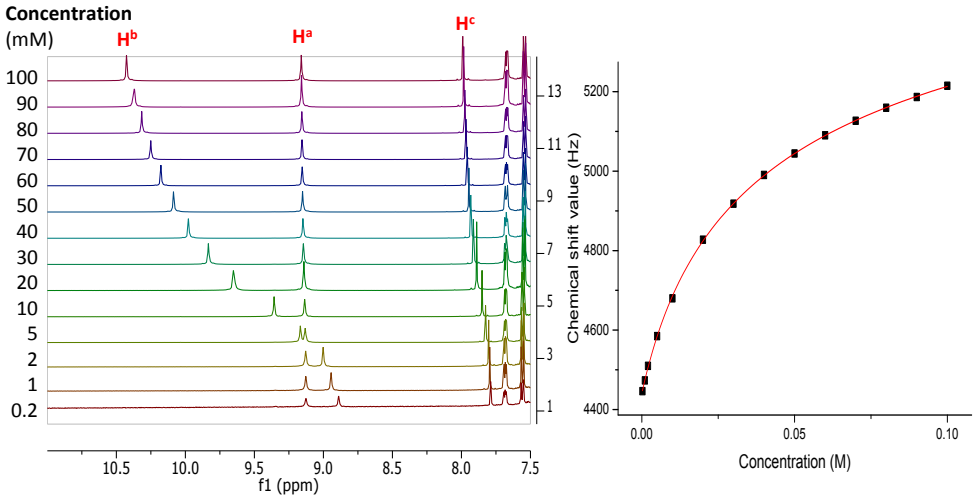


## *Catalyst 3b*

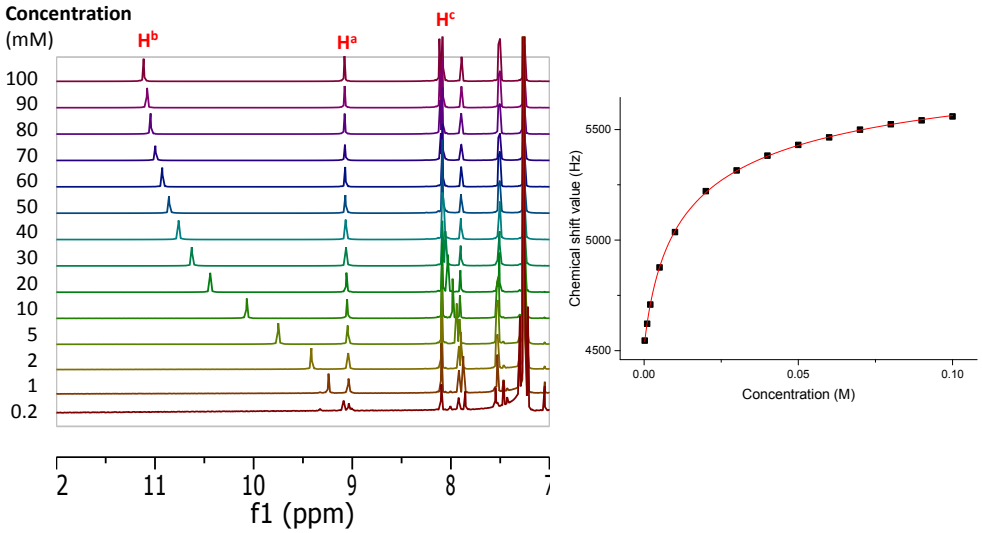

## Binding Studies

Job plots confirming 1:1 binding stoichiometry between catalyst **1c** and either **DHP**, 4-methoxyphenol, or benzoic acid were made:[5]

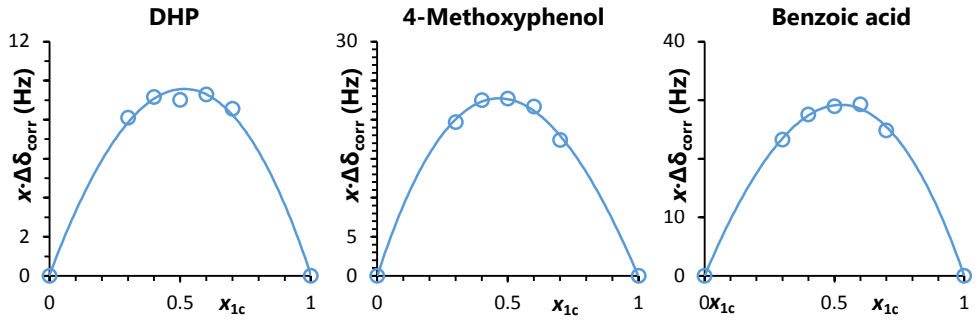


Keeping a constant concentration of **1c** (1.0 mM) the two guests were titrated into this **1c** solution. The change in chemical shift was fitted to the following equation (fitted parameters in blue):

$$\Delta\delta = \frac{\Delta\delta_{max}}{[H]_0} \cdot \frac{\left([G]_0 + [H]_0 + K_a^{-1}\right) - \sqrt{\left([G]_0 + [H]_0 + K_a^{-1}\right)^2 - 4[G]_0[H]_0}}{2}$$

where $\Delta\delta_{max}$ is the maximal change in chemical shift. $K_a$ is the binding constant.[6]

Since both of the guests contained hydrogen bond donors/acceptors and due to the labile nature of the NH protons, binding constants were determined by fitting to the changes in chemical shifts for $H^c$ (see designations in Figure S 10). Nevertheless, fitting to the changes in chemical shifts for $H^b$ gave similar results.

***Table S6: Binding Constants Between Catalyst 1c and DHP, 4-Methoxyphenol, or Benzoic Acid***

| | $K_a$ ($M^{-1}$)[a] | |
|---|---|---|
| **Guest** | Proton b[b] | Proton c[b] |
| **DHP** | *c.n.d.*[c] | *c.n.d.* |
| **4-Methoxyphenol** | 1.32 ± 0.03 | 1.71 ± 0.03 |
| **Benzoic Acid** | 46 ± 4 | 52 ± 4 |

Determined by $^1$H NMR spectroscopy in $CDCl_3$ at 20 °C. [a] As obtained from fit to the chemical shift changes of the proton indicated. Errors given are standard errors on best fit. [b] Protons are named according to Figure S 10. [c] A value of (0.49 ± 0.02) $M^{-1}$ could be obtained from these data, however since a $[G]_0/[H]_0$ ratio of more than 1000 was necessary, the data is not fit for $K_a$ determination.[5] *c.n.d.*: Could not be determined.

Though catalyst **1c** only binds 4-methoxyphenol with a relatively low binding constant, it was evident that the interaction between catalyst **1c** and **DHP** was even lower ($K_a$ was found to be below what can be determined by NMR, e.g. below ca. 1 $M^{-1}$).[5]

[5] P. Job, *Annales de Chimie (Paris)*, 1928, **9**, 113.
[6] K. Hirose, *Analytical Methods in Supramolecular Chemistry*, ed. C. Schalley, Wiley-VCH Verlag GmbH & Co. KGaA, 2007.

Catalyst **1c** was found to bind benzoic acid stronger than both of the abovementioned, albeit still weakly, but this confounding fact cannot in itself explain the overall improvement on the reaction rate in the presence of this acid. A likely coupling between the observed benzoic acid-catalyst interaction and the observed increase in reaction rate, could be that the chemical shift changes in the NMR experiment are the result of benzoic acid interacting in an electrophilic manner with the catalyst, maybe in the form of partial protonation of the imine nitrogen. Such an interaction would result in a more electron-deficient, and thus better, catalyst.

Data for the titration of catalyst **1c** with **DHP**, 4-methoxyphenol, and benzoic acid, respectively, is shown below.

### *Catalyst 1c with DHP*

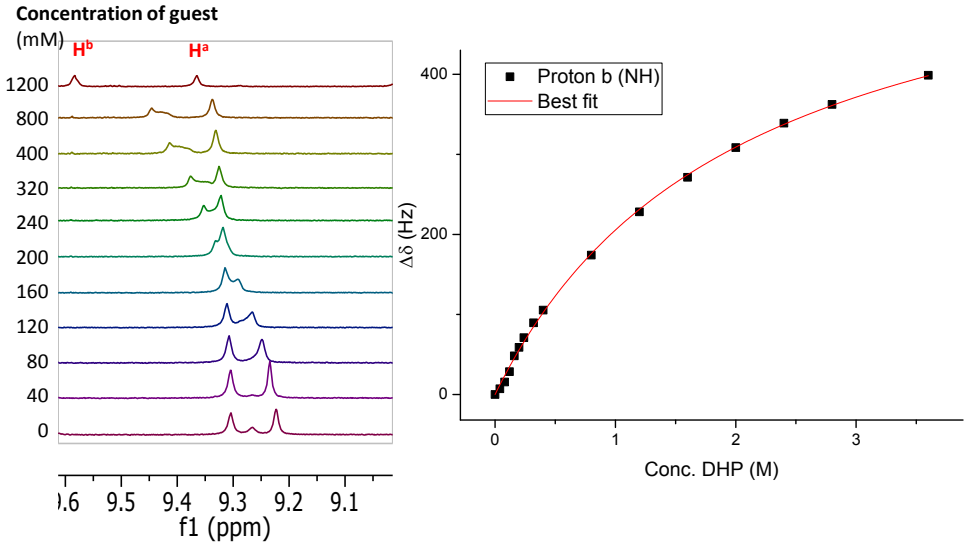


Note: Very large excess (4000 eq. of DHP) was added, putting these measurements outside the range in which $^{1}$H NMR can give proper determinations of $K_a$.[5]

### *Catalyst 1c with 4-methoxyphenol*

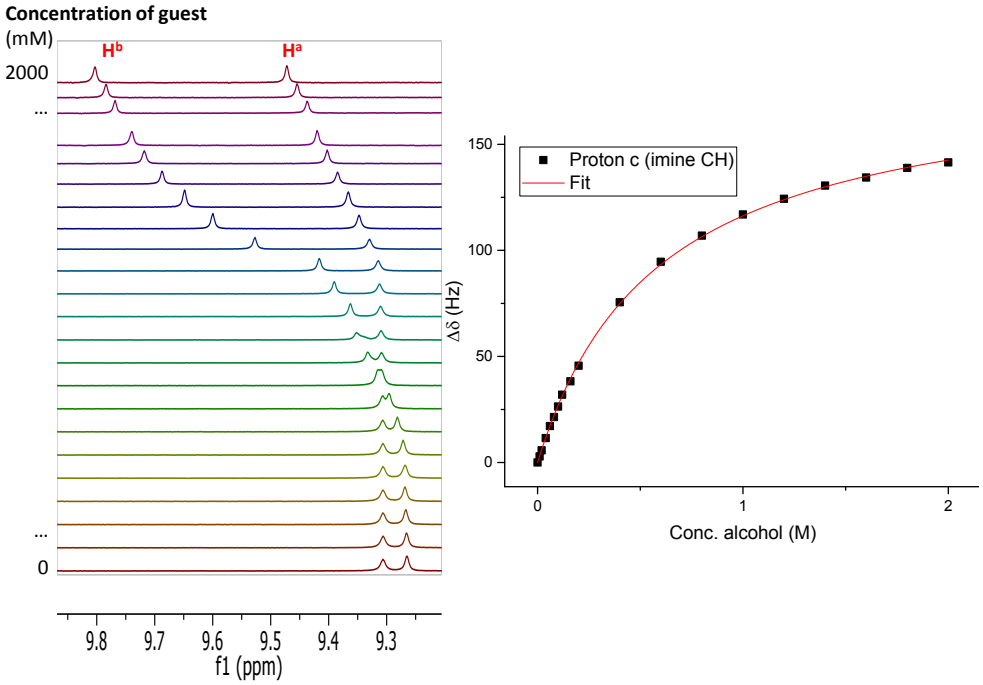


### *Catalyst 1c with benzoic acid*

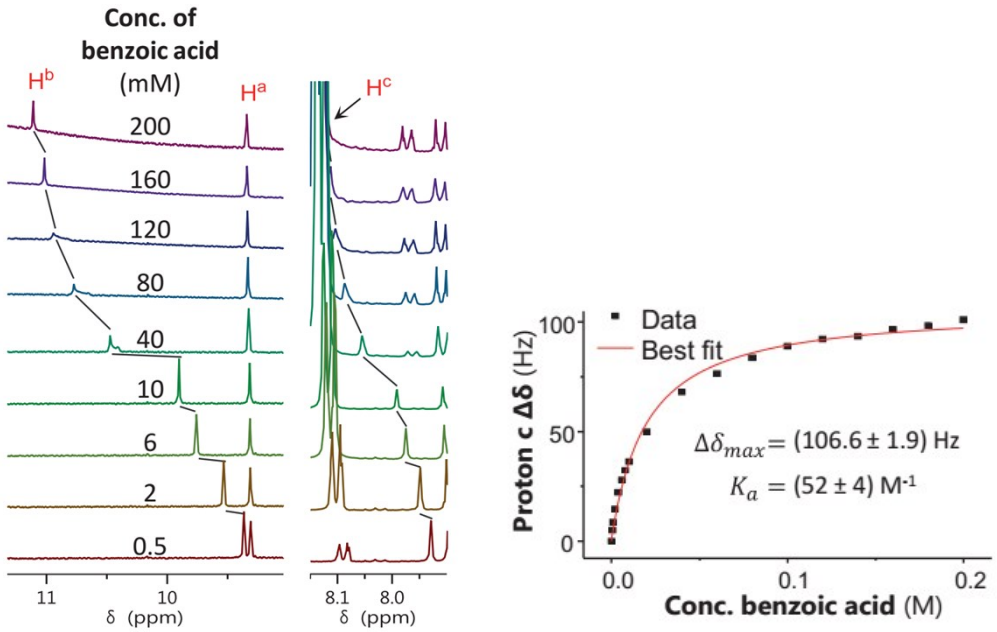

# 8. Determination of p$K_a$ of Catalyst 1c in DMSO

A modification of the overlapping indicator method was applied.[7] In this modification, catalyst **1c** functioned as the indicator, while benzoate (or acetate) was used as the base (B in the scheme below). Deprotonation of catalyst **1c** (AH in the general scheme below) results in formation of a red solution.

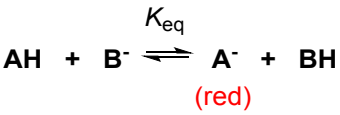


(0.1 mM in DMSO)

**1c** **1c** + $AcO^-$ (5 eq.)

Note that it follows that $K_{eq} = K_{a(AH)} \cdot K_{a(BH)}^{-1}$.

The rise in absorbance at ca. 500 nm was used as indication of the degree of deprotonation:

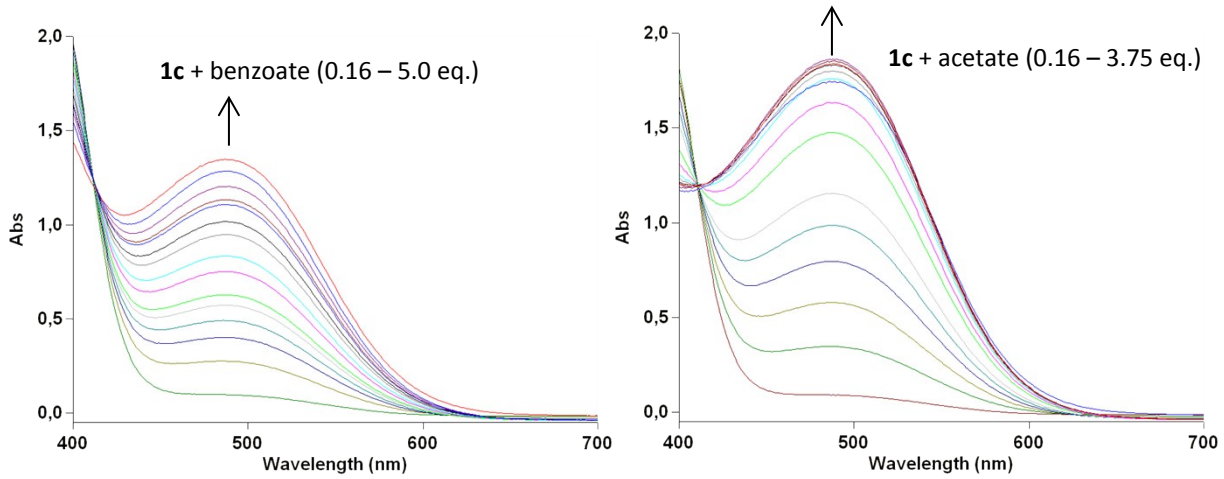


By applying excess base, a titration curve from which $K_{eq}$ can be determined by non-linear regression to the following equation (see below for elucidation of this equation) arises:

$$Abs = \frac{Abs_{max}\left([AH]_0 + [B]_0 - \sqrt{([AH]_0 + [B]_0)^2 - 4\left(1 - {K_{eq}}^{-1}\right)[AH]_0 \cdot [B]_0}\right)}{2[AH]_0 - 2[AH]_0 \cdot {K_{eq}}^{-1}}$$

*Abs* is the measured absorbance (at a wavelength of 500 nm in this case), which is plotted as a function of added base ($[B]_0$), while the concentration of acid (**1c**), $[AH]_0$, is maintained constant (0.10 mM in this experiment). The maximum absorbance, $Abs_{max}$, and $K_{eq}$ is found by fitting to the equation above (red line):

[7] W. S. Matthews, J. E. Bares, J. E. Bartmess, F. G. Bordwell, F. J. Cornforth, G. E. Drucker, Z. Margolin, R. J. McCallum, G. J. McCollum and N. R. Vanier, *J. Am. Chem. Soc.*, 1975, **97**, 7006.

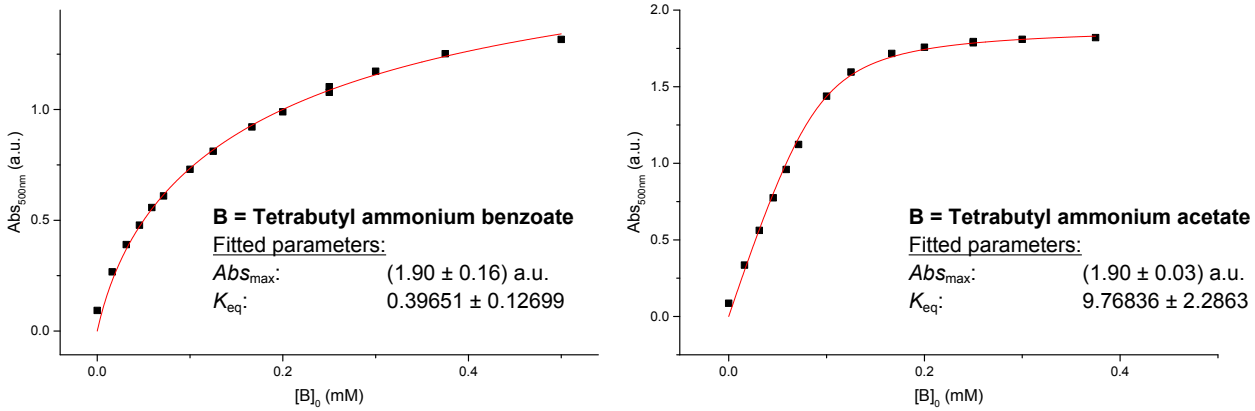


The p$K_a$ value of AH (**1c**) is given by:

$$pK_{a(AH)} = pK_{a(BH)} - \log(K_{eq})$$

By exploiting that the p$K_a$ values of benzoic acid and acetic acid in DMSO (11.1 and 12.6, resp.)[8] are known, one easily arrives at the following values (error based on propagation of error on $K_{eq}$ assuming no error on p$K_{a(BH)}$ literature values):

Titration with benzoate: p$K_{a(\mathbf{1c})}$ = 11.5 ± 0.1
Titration with acetate: p$K_{a(\mathbf{1c})}$ = 11.6 ± 0.1

These two values are identical, within error. The number from the titration with benzoate is deemed to be the most reliable, since the overlapping indicator method is most reliable with indicators that are close to the substrate in p$K_a$ value.

**Elucidation of equation used to identify $K_{eq}$ by non-linear regression:**
Consider the following reaction:

| | **AH** | **+** | **B$^-$** | ⇌ | **A$^-$** | **+** | **BH** |
|---|---|---|---|---|---|---|---|
| Concentration: | | | | | | | |
| At $t_0$: | $[AH]_0$ | | $[B]_0$ | | 0 | | 0 |
| At equilibrium: | $[AH]_0 - x$ | | $[B]_0 - x$ | | $[A] = x$ | | $[BH] = x$ |

When this reaction is monitored by the UV/vis absorbance of **A$^-$**, it follows from Lambert-Beer's law that

$$x = \frac{Abs}{Abs_{max}}[AH]_0$$

if monitored at a wavelength where only **A$^-$** absorbs.

The equilibrium constant for the reaction is given by:

[8] F. G. Bordwell, *Acc. Chem. Res.*, 1988, **21**, 456.

$$K_{eq} = \frac{[A][BH]}{[AH][B]} = \frac{x^2}{([AH]_0 - x)([B]_0 - x)}$$

This is easily rewritten to:

$$0 = \left(1 - K_{eq}^{-1}\right)x^2 - \left([AH]_0 + [B]_0\right)x + [AH]_0[B]_0$$

This quadratic equation has two (non-complex) solutions:

$$x = \frac{[AH]_0 + [B]_0 + \sqrt{\left([AH]_0 + [B]_0\right)^2 - 4\left(1 - K_{eq}^{-1}\right)[AH]_0[B]_0}}{2(1 - K_{eq}^{-1})} \quad \text{(Eq. 1)}$$

*and*

$$x = \frac{[AH]_0 + [B]_0 - \sqrt{\left([AH]_0 + [B]_0\right)^2 - 4\left(1 - K_{eq}^{-1}\right)[AH]_0[B]_0}}{2(1 - K_{eq}^{-1})} \quad \text{(Eq. 2)}$$

To identify the proper solution (within non-imaginary numbers), we utilise the real-life criteria:

$0 < x \leq [AH]_0$

$[B]_0 > 0$

$K_{eq} > 0$

The final criterion specifies that there must be a (non-complex) solution also for $0 < K_{eq} < 1$, since this is a subset of $K_{eq} > 0$. Any $K_{eq}$ between 0 and 1 results in a negative denominator in both Eq.'s 1 and 2. Since $[AH]_0 + [B]_0$ is larger than zero (based on the real-life criteria), Eq. 1 cannot give a value of $x > 0$ for $0 < K_{eq} < 1$. Thus, only Eq. 2 can give (non-complex) solutions for all $K_{eq} > 0$, and therefore is the only equation that meets all of the real-life criteria.

Substituting $x = \frac{Abs}{Abs_{max}}[AH]_0$ and rearranging, one arrives at the final equation

$$Abs = \frac{Abs_{max}\left([AH]_0 + [B]_0 - \sqrt{\left([AH]_0 + [B]_0\right)^2 - 4\left(1 - {K_{eq}}^{-1}\right)[AH]_0 \cdot [B]_0}\right)}{2[AH]_0 - 2[AH]_0 \cdot {K_{eq}}^{-1}}$$

which describes the relationship between absorbance, $Abs$, and starting concentration of base, $[B]_0$, and makes it possible to identify *via* non-linear regression the equilibrium constant, $K_{eq}$, provided that the starting concentration of acid, $[AH]_0$, is kept constant.

# 9. Crystal Structure Data

All single crystal X-ray diffraction data were collected on a Bruker D8 Venture equipped with a IμS microfocus source, a KAPPA goniometer, a nitrogen cryostream cooling device and a PHOTON 100 detector, using Mo-$K_\alpha$ radiation. The structures were solved using direct methods (SHELXS97 or SHELXS as implemented in APEX2) and refined using the SHELXL2013 software package.[9]

***3,5-Bis(trifluoromethyl)benzaldehyde 4-(3,5-bistrifluoromethylphenyl)thiosemicarbazone (1b):***
$C_{18}H_9F_{12}N_3S$; M = 527.34; Monoclinic; a = 4.7617(3) Å, b = 31.515(3) Å, c = 13.2597(10) Å, α = 90°, β = 92.153(3)°, γ = 90°; V = 1988.4(3) Å$^3$; T = 122.15 K; space group $P2_1/c$ ; Z = 4; μ(Mo-$K_\alpha$) = 0.07 mm$^{-1}$; 11333 reflections measured, 3629 independent reflections ($R_{int}$ = 0.156). The final $R_1$ value was 0.053 [$F^2 > 2\sigma(F^2)$]. The final $R_1$ value was 0.072 (all data). The final $wR(F^2)$ (all data) value was 0.121, The goodness of fit on $F^2$ was 1.06.

An electronic version of the refined structure has been deposited with the Cambridge Structural Database: CSD-1473889.

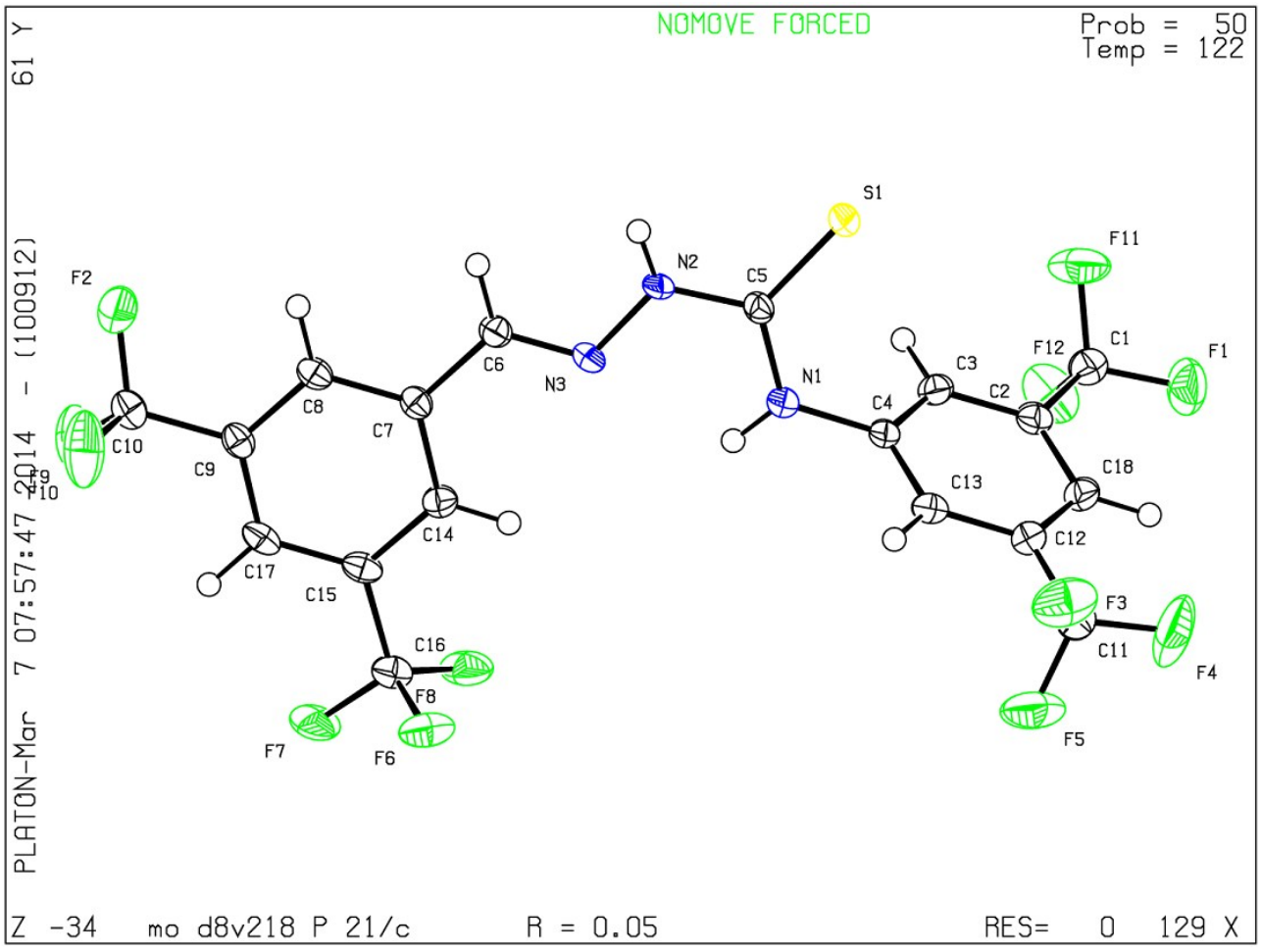


[9] G. Sheldrick, *Acta Crystallogr. Sect. A*, 2008, **64**, 112.

***4-Nitrobenzaldehyde 4-(3,5-Bistrifluoromethylphenyl)thiosemicarbazone (1c):***

$C_{16}H_{10}F_6N_4O_2S$; M = 436.34; Monoclinic; a = 12.2715(14) Å, b = 8.4441(10) Å, c = 16.4877(19) Å, α = 90°, β = 93.794(4)°, γ = 90°; V = 1704.7(3) Å$^3$; T = 122 K; space group $P2_1/c$; Z = 4; μ(Mo-$K_\alpha$) = 0.07 mm$^{-1}$; 23827 reflections measured, 3029 independent reflections ($R_{int}$ = 0.070). The final R1 value was 0.0575 [$F^2 > 2\sigma(F^2)$]. The final $R_1$ value was 0.0736 (all data). The final $wR(F^2)$ (all data) value was 0.1555. The goodness of fit on $F^2$ was 1.031.

An electronic version of the refined structure has been deposited with the Cambridge Structural Database: CSD-1473890.

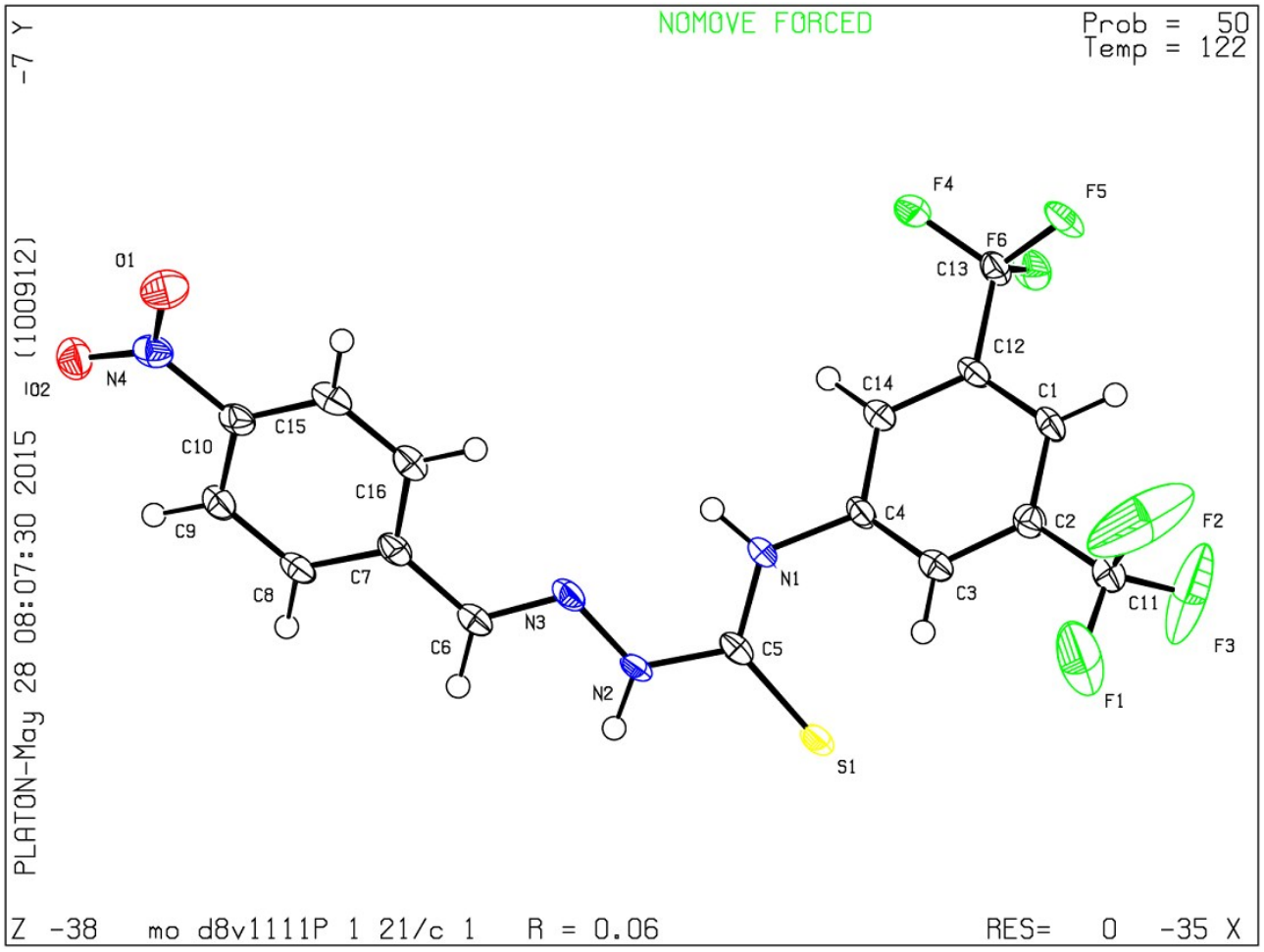

***2,4-Dinitrobenzaldehyde 4-(3,5-Bistrifluoromethylphenyl)thiosemicarbazone (1d):***

$C_{16}H_9F_6N_5O_4S$; M = 481.34; Triclinic; a= 8.8724(4) Å, b = 9.8446(5) Å, c = 12.3483(6) Å, α = 89.810(2)°, β = 71.081(2)°, γ = 68.037(2)°; V = 937.66(8) Å$^3$; T = 295 K; space group P-1 ; Z = 2; μ(Mo-$K_\alpha$) = 0.07 mm$^{-1}$; 21041 reflections measured, 3830 independent reflections ($R_{int}$ = 0.0330). The final $R_1$ value was 0.0403 [$F^2 > 2\sigma(F^2)$]. The final $R_1$ value was 0.0523 (all data). The final $wR(F^2)$ (all data) value was 0.1115. The goodness of fit on $F^2$ was 1.035.

An electronic version of the refined structure has been deposited with the Cambridge Structural Database: CSD- 1473916.

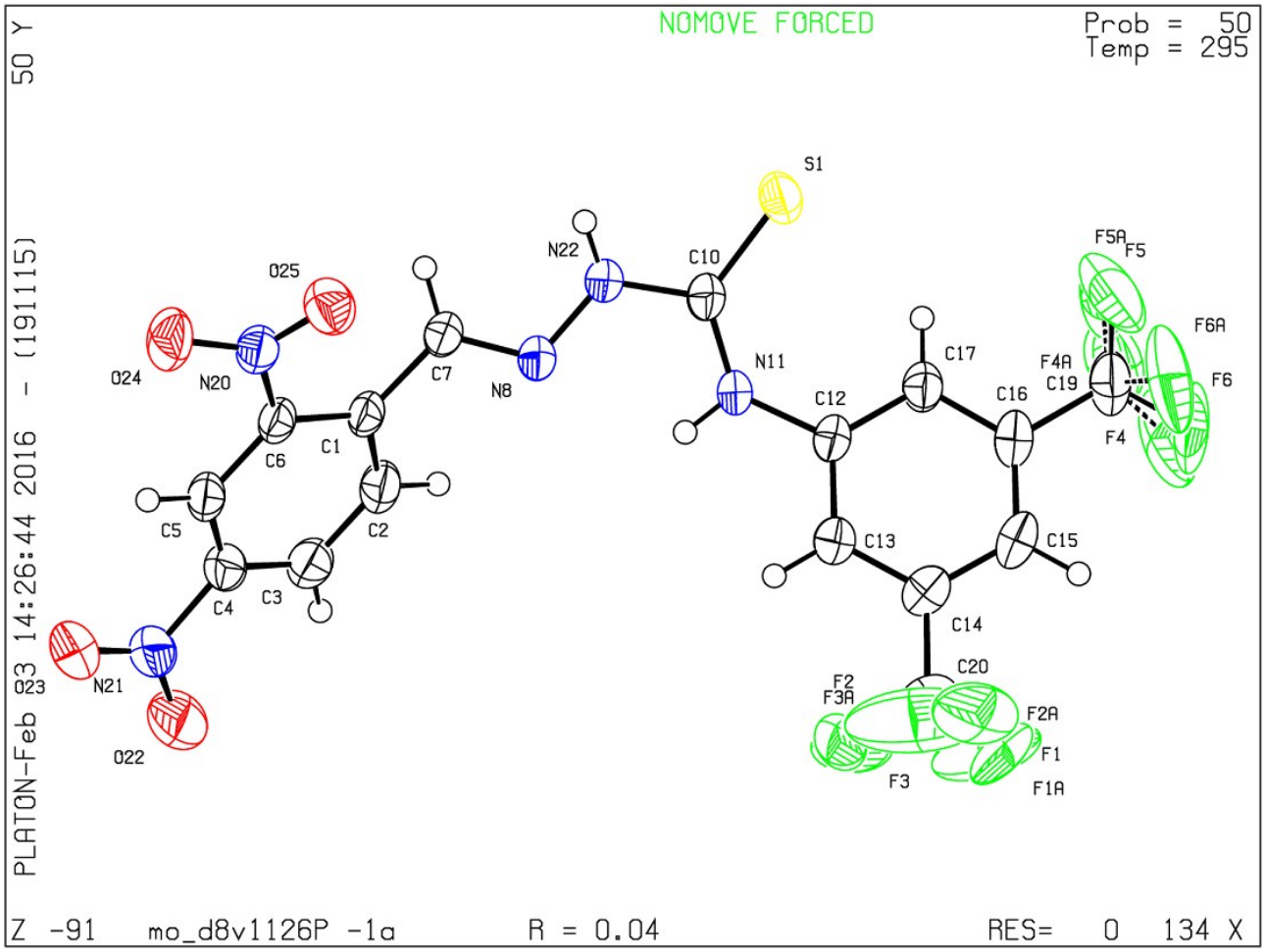

***4-(Methoxycarbonyl)benzaldehyde 4-(3,5-Bistrifluoromethylphenyl)thiosemicarbazone (1h):***
$C_{18}H_{13}F_6N_3O_2S$; M = 449.37; Monoclinic; a = 12.2731(16) Å, b = 9.2592(14) Å, c = 16.180(3) Å, α = 90°, β = 91.897(5)°, γ = 90°; V = 1837,7(5) Å$^3$; T = 100(30) K; space group $P2_1/c$; Z = 4; μ(Mo-$K_\alpha$) = 0.07 mm$^{-1}$; 22854 reflections measured, 3785 independent reflections ($R_{int}$ = 0.0585). The final $R_1$ value was 0.0366 [$F^2 > 2\sigma(F^2)$]. The final $R_1$ value was 0.0447 (all data). The final $wR(F^2)$ (all data) value was 0.0907. The goodness of fit on $F^2$ was 1.040.

An electronic version of the refined structure has been deposited with the Cambridge Structural Database: CSD-1473891.

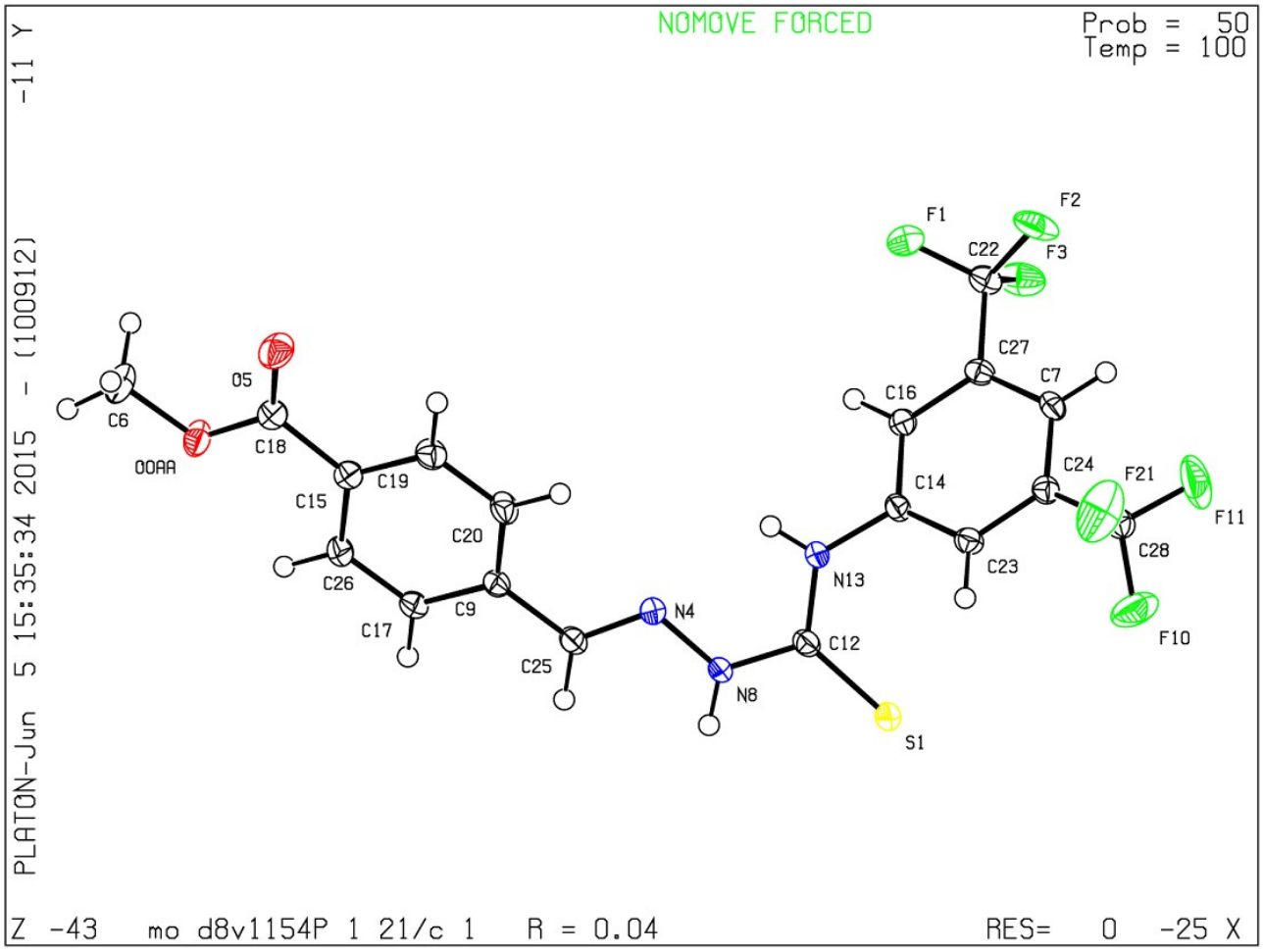

## Crystal Structures Show Dimer Formation in the Solid State

All of the crystal structures show the same characteristic overall structure (figure s **11** and figure s **12**): Intramolecular hydrogen bonding fixes the thiosemicarbazone moiety in an *s*-trans configuration about the $C^3$-$N^2$ bond. Furthermore, the hydrogen-bond donor/acceptor array presented in this configuration forms intermolecular hydrogen bonds to a neighbouring thiosemicarbazone molecule facing in the opposite direction.

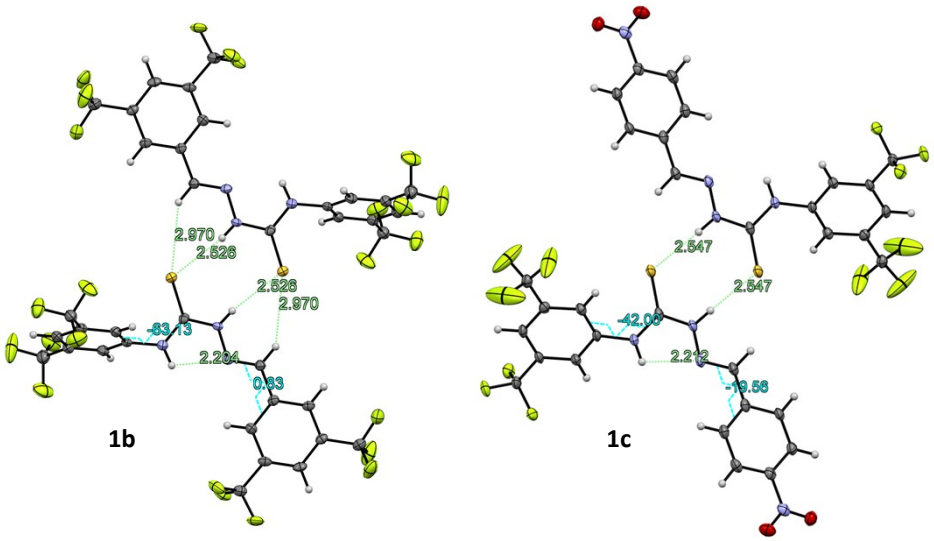


**Figure S 11:** Crystal structures (50 % probability ellipsoids) showing dimers of catalysts **1b** grown from ethanol (left) and **1c** grown from $CH_2Cl_2$/methanol (right). Torsional angles between aromatic rings and the central thiosemicarbazone moiety (cyan) and hydrogen bonds shorter than 3 Å (green) are shown.

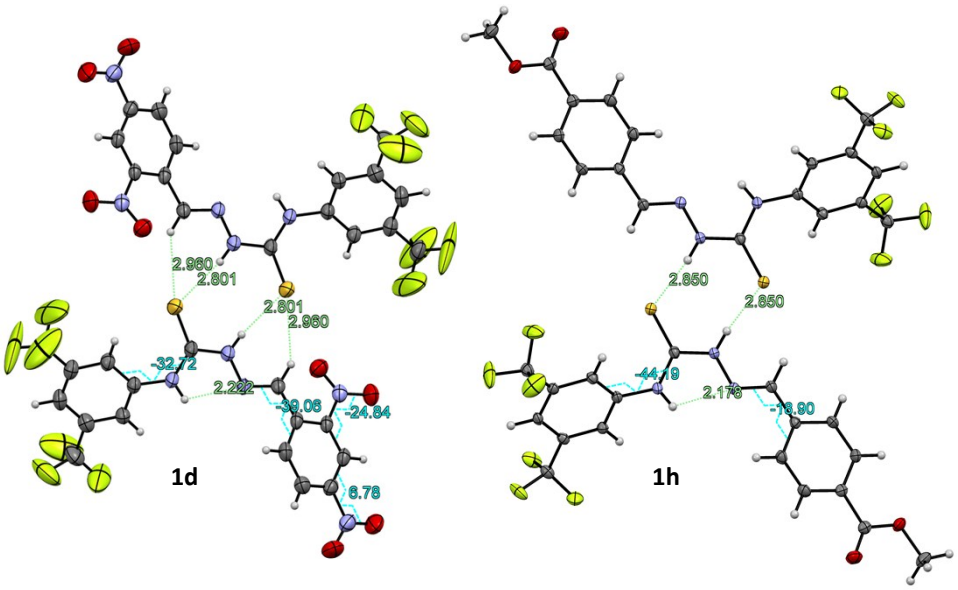


**Figure S 12:** Crystal structures (50 % probability ellipsoids) showing dimers of catalysts **1d** (left) and **1h** (right) grown from ethanol (disordered $CF_3$ groups omitted for clarity). Torsional angles between aromatic rings and the central thiosemicarbazone moiety (cyan) and hydrogen bonds shorter than 3 Å (green) are shown.

The thiourea *N*-phenyl is twisted out of the plane of the thiosemicarbazone moiety by 33 – 63 degrees, presumably because of steric clash between the *ortho*-hydrogen and the thionyl sulfur atom. The imine *C*-phenyl is twisted only 1 – 20 degrees out of the plane of the thiosemicarbazone moiety, except in **1d**,

where the torsional angle is 39 degrees. Presumably, the steric demand of the *ortho*-nitro group causes this enhancement of the torsional angle in **1d**.

None of the crystals contained any solvent molecules bound in the crystal lattice, though weak interactions with alcohols were seen in $CDCl_3$ solution (see NMR titrations above). Catalyst **1c** was also grown from nitromethane, but this structure was practically identical to the one obtained from $CH_2Cl_2$/methanol, and these crystals did not incorporate solvent molecules either.

# 10. Synthetic Procedures

### *1-Isothiocyanato-3,5-bis(trifluoromethyl)benzene[10]:*

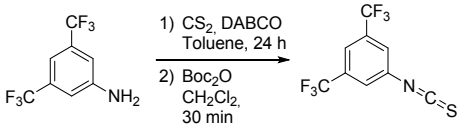


3,5-Bis(trifluoromethyl)aniline (3.1 mL, 20 mmol) and DABCO (2.69 g, 24 mmol) were dissolved in toluene (60 mL) and $CS_2$ (3.62 mL, 60 mmol) was added. After stirring at room temperature for 24 hours, the reaction mixture was cooled on an ice-bath and the precipitate was collected and washed with ice-cold toluene. The precipitate was redissolved in $CH_2Cl_2$ and while cooling on an ice-bath, di-*tert*-butyl dicarbonate (4.80 g, 22 mmol) dissolved in $CH_2Cl_2$ (30 mL) was added. The reaction mixture was heated gently until gas evolution had ceased and then volatiles were removed *in vacuo*. The crude product was used without further purification.

### *4-(3,5-Bis(trifluoromethyl)phenyl)thiosemicarbazide (1):*

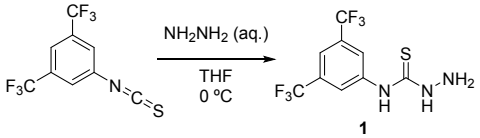


**1**

Hydrazine hydrate (50 – 60 %, 32 mL) was diluted with THF (80 mL) and while cooling the reaction mixture in an ice-bath, 1-isothiocyanato-3,5-bis(trifluoromethyl)benzene (3.7 mL, 20 mmol) dissolved in THF (20 mL) was added over fifteen minutes. The reaction mixture was diluted with $CH_2Cl_2$ (100 mL) and washed with water (3 x 80 mL). The resulting aqueous phase was extracted once with $CH_2Cl_2$ (80 mL) and the combined organic phases were dried ($Na_2SO_4$) and concentrated *in vacuo*. Recrystallization from ethanol (96 %, 6 mL) yielded 4.30 g of the title compound (71 %).

Melting point: 158 – 160 °C (lit.: 158 – 160 °C, MeOH/$H_2O$)[11]. Elemental analysis for $C_9H_7F_6N_3S$: Found (calculated): 35.64 % C (35.65); 1.96 % H (2.33); 13.72 % N (13.86). $^1$H NMR (500 MHz, $CDCl_3$) δ = 9.54 (bs, 1H), 8.25 (s, 2H), 7.68 (s, 1H), 7.63 (bs, 1H), 4.03 (bs, 2H). $^{13}$C NMR (126 MHz, $CDCl_3$) δ = 181.17, 139.58, 132.11 (q, *J*=33.6), 123.31 (q, *J*=3.7), 123.19 (q, *J*=272.8), 118.92 (hept, *J*=3.9). $^{19}$F NMR (282 MHz, $CDCl_3$) δ = -61.78. HRMS: (ESI+) Calculated for $C_9H_8F_6N_3S^+$: 304.0338, found: 304.0341.

### *Benzaldehyde 4-(3,5-Bistrifluoromethylphenyl)thiosemicarbazone (1a):*

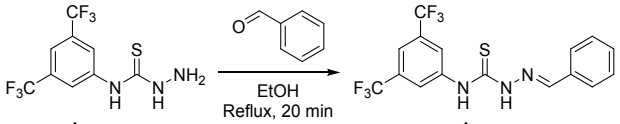


**1** **1a**

Thiosemicarbazide **1** (758 mg, 2.50 mmol) was dissolved in ethanol (96 %, 10 mL) and benzaldehyde (1.02 mL, 10 mmol) was added. While stirring, the reaction was heated to reflux for 10 minutes and then all volatiles were removed *in vacuo*. Recrystallization from boiling ethanol (96 %, 6 mL) yielded a white fibrous solid, 818 mg (84 %).

Melting point: 195 – 196 °C. Elemental analysis for $C_{16}H_{11}F_6N_3S$: Found (calculated) 49.25 % C (49.11); 2.43 % H (2.83); 10.65 % N (10.74). $^1$H NMR (500 MHz, $CDCl_3$) (Note: All signals are broad because of rotational isomers) δ = 9.56 (s, 1H), 9.39 (s, 1H), 8.29 (s, 2H), 7.92 (s, 1H), 7.77 – 7.67 (m, 3H), 7.51 – 7.42 (m, 3H). $^{13}$C NMR (126 MHz, $CDCl_3$) δ = 175.80, 144.04, 139.46, 132.53, 132.22 (q, *J*=33.7), 131.45, 129.23, 127.82, 123.88 (q, *J*=3.8), 123.18 (q, *J*=272.8), 119.37 (hept, *J*=4.4). $^{19}$F NMR (282 MHz, $CDCl_3$) δ = -61.75. HRMS: (ESI+) Calculated for $C_{16}H_{12}F_6N_3S^+$: 392.0651, found: 392.0655.

---

[10] J. Yao, J. Chen, Z. He, W. Sun and W. Xu, *Biorg. Med. Chem.*, 2012, **20**, 2923.

[11] K. Nagarajan, P. K. Talwalker, C. L. Kulkarni, A. Venkateswarlu, S. S. Prabhu and G. V. Nayak, *Indian J. Chem., Sect. B: Org. Chem. Incl. Med. Chem.*, 1984, **23**, 1243.

### *3,5-Bis(trifluoromethyl)benzaldehyde 4-(3,5-Bistrifluoromethylphenyl)thiosemicarbazone (1b):*

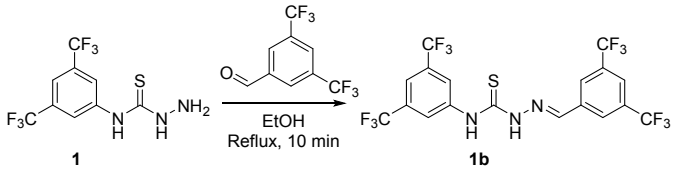


1 1b

Thiosemicarbazide **1** (303 mg, 1.00 mmol) was dissolved in ethanol (96 %, 4 mL) and 3,5-bis(trifluoromethyl)benzaldehyde (164 µL, 1.05 mmol) was added. While stirring, the reaction was heated until boiling and approximately half of the volume was allowed to evaporate. The reaction mixture was cooled in an ice-bath and the precipitate was collected and recrystallized from boiling ethanol (96 %, 1 mL) to give a white powder that was air-dried. Yield: 459 mg (87 %).

Melting point: 207 – 208 °C. Elemental analysis for $C_{18}H_9F_{12}N_3S$: Found (calculated) 41.02 % C (41.00); 1.29 % H (1.79), 7.88 % N (7.97). $^1$H NMR (20 mM, 500 MHz, $CDCl_3$) (Note: All signals are broad singlets because of rotational isomers) δ = 9.96 (s, 1H), 9.22 (s, 1H), 8.21 (s, 2H), 8.12 (s, 2H), 8.02 (s, 1H), 7.96 (s, 1H), 7.79 (s, 1H). $^{13}$C NMR (20 mM, 126 MHz, $CDCl_3$) δ = 176.44, 140.35, 139.00, 134.78, 132.91 (q, *J*=34.0), 132.43 (q, *J*=33.9), 127.34 (q, *J*=4.1), 125.02 (q, *J*=4.3), 124.35 (hept., *J*=3.2), 123.08 (q, *J*=273.0), 123.00 (q, *J*=273.0), 120.19 (hept., *J*=3.7). $^{19}$F NMR (282 MHz, $CDCl_3$) δ -61.72 (s, 6F), -61.82 (s, 6F). HRMS: (ESI+) Calculated for $C_{18}H_{10}F_{12}N_3S^+$: 528.0398, found: 528.0422.

### *4-Nitrobenzaldehyde 4-(3,5-Bistrifluoromethylphenyl)thiosemicarbazone (1c):*

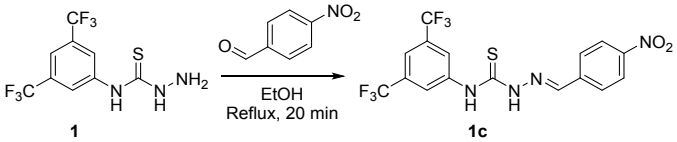


1 1c

Thiosemicarbazide **1** (760 mg, 2.51 mmol) was dissolved in ethanol (96 %, 10 mL) and 4-nitrobenzaldehyde (0.56 g, 3.75 mmol) was added. While stirring, the reaction mixture was heated until boiling and approximately half of the volume was allowed to evaporate. The reaction mixture was cooled in an ice-bath, and the yellow precipitate was collected and air-dried. Yield: 817 mg (80 %).

Melting Point: 207 – 208 °C. Elemental analysis for $C_{16}H_{10}F_6N_4O_2S$: Found (calculated) 44.44 % C (44.04); 2.02 % H (2.31), 12.73 % N (12.84). $^1$H NMR (500 MHz, DMSO-$d_6$) δ = 12.47 (s, 1H), 10.65 (s, 1H), 8.46 (s, 2H), 8.29 (s, 1H), 8.28 (d, *J*=8.6, 2H), 8.20 (d, *J*=8.6, 2H), 7.92 (s, 1H). $^{13}$C NMR (126 MHz, DMSO-$d_6$) δ = 176.38, 147.96, 141.58, 140.92, 140.11, 129.89 (q, *J*=33.0), 128.69, 125.67, 123.83, 123.24 (q, *J*=272.8), 118.27. $^{19}$F NMR (282 MHz, DMSO-$d_6$) δ = -59.72. HRMS: (ESI+) Calculated for $C_{16}H_{11}F_6N_4O_2S^+$: 437.0501, found: 437.0491.

### *2,4-Dinitrobenzaldehyde 4-(3,5-Bistrifluoromethylphenyl)thiosemicarbazone (1d):*

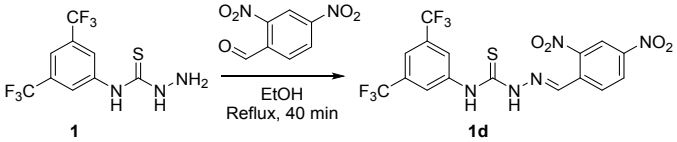


1 1d

Thiosemicarbazide **1** (760 mg, 2.51 mmol) was dissolved in ethanol (96 %, 40 mL) and 2,4-dinitrobenzaldehyde (0.74 g, 3.75 mmol) was added. While stirring, the reaction was heated until boiling and approximately half of the volume was allowed to evaporate. The reaction mixture was cooled in an ice-bath, and the yellow flaky precipitate was collected and air-dried. Yield: 1.02 g (85 %).

Melting Point: 211 – 215 °C (dec.). Elemental analysis for $C_{16}H_9F_6N_5O_4S$: Found (calculated) 40.23 % C (39.93); 1.60 % H (1.88), 14.46 % N (14.55). $^1$H NMR (500 MHz, DMSO-$d_6$) δ = 12.70 (s, 1H), 10.74 (s, 1H), 8.83 (d, *J*=9, 1H), 8.79 (d, *J*=2, 1H), 8.69 (s, 1H), 8.55 (dd, *J*=9, 2, 1H), 8.44 (s, 2H), 7.94 (s, 1H). $^{13}$C NMR (126 MHz, DMSO-$d_6$) δ = 176.73, 148.04, 147.32, 140.80, 137.58, 133.91, 129.97 (q, *J*=33.0), 129.88, 127.16, 125.75, 123.20 (q, *J*=272.8), 120.42, 118.50. $^{19}$F NMR (282 MHz, DMSO-$d_6$) δ = -59.68. HRMS: (ESI+) Calculated for $C_{16}H_{10}F_6N_5O_4S^+$: 482.0352, found: 482.0336.

### *Pentafluorobenzaldehyde 4-(3,5-Bistrifluoromethylphenyl)thiosemicarbazone (1e):*

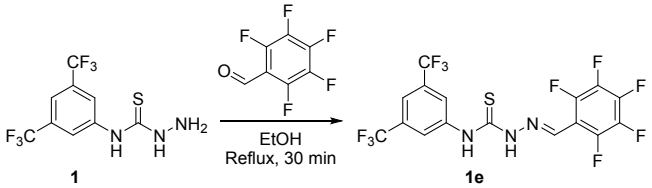


1 1e

Thiosemicarbazide **1** (759 mg, 2.50 mmol) was dissolved in ethanol (96 %, 20 mL) and pentafluorobenzaldehyde (0.47 mL, 3.75 mmol) was added. While stirring, the reaction mixture was heated until boiling and approximately half of the volume

was allowed to evaporate. The reaction mixture was cooled in an ice-bath, and a white fibrous precipitate was collected. After evaporation of further solvent until a total volume of ca. 5 mL, it was possible to isolate another batch of compound. The two harvests were combined and air-dried. Yield: 1.039 g (86 %).

Melting Point: 192 – 193 °C. Elemental analysis for $C_{16}H_6F_{11}N_3S$: Found (calculated) 40.17 % C (39.93); 0.94 % H (1.26), 8.63 % N (8.73). $^1$H NMR (500 MHz, DMSO-$d_6$) δ = 12.49 (s, 1H), 10.33 (s, 1H), 8.42 (s, 2H), 8.28 (s, 1H), 7.90 (s, 1H). $^{13}$C NMR (126 MHz, DMSO-$d_6$) δ = 176.43, 144.67 (dm, *J*=254.7), 140.93 (dm, *J*=254.0), 140.76, 137.33 (dm, *J*=245.3), 131.94, 129.93 (q, *J*=33.0), 125.07, 123.19 (q, *J*=272.7), 118.14, 109.37. $^{19}$F NMR (282 MHz, DMSO-$d_6$) δ = -59.74 (s, 6F), -139.48 (d, *J*=19, 2F), -150.70 (t, *J*=22, 1F), -160.82 (t, *J*=20, 2F). HRMS: (ESI+) Calculated for $C_{16}H_7F_{11}N_3S^+$: 482.0180, found: 482.0177.

### *2-Formylpyridine 4-(3,5-Bistrifluoromethylphenyl)thiosemicarbazone (1f):*

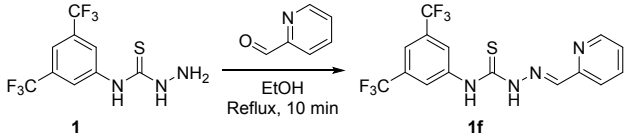


1 1f

Thiosemicarbazide **1** (758 mg, 2.50 mmol) was dissolved in ethanol (96 %, 10 mL) and 2-formylpyridine (0.36 mL, 3.75 mmol) was added. While stirring, the reaction mixture was heated until boiling and approximately half of the volume was allowed to evaporate. The reaction mixture was cooled in an ice-bath, and the light yellow precipitate was collected and air-dried. Yield: 904 mg (91 %).

Melting Point: 192 – 193 °C. Elemental analysis for $C_{15}H_{10}F_6N_4S$: Found (calculated) 46.27 % C (45.92), 2.31 % H (2.57), 14.22 % N (14.28). $^1$H NMR (500 MHz, DMSO-$d_6$) δ = 12.41 (s, 1H), 10.60 (s, 1H), 8.62 (d, *J*=4.9, 1H), 8.47 (s, 2H), 8.43 (d, *J*=8.0, 1H), 8.25 (s, 1H), 7.97 – 7.86 (m, 2H), 7.43 (dd, *J*=7.4, 4.9, 1H). $^{13}$C NMR (126 MHz, DMSO-$d_6$) δ = 176.24, 152.80, 149.50, 144.39, 140.92, 136.59, 129.85 (q, *J*=33.1), 125.56, 124.57, 123.24 (q, *J*=272.9), 120.73, 118.20. $^{19}$F NMR (282 MHz, DMSO-$d_6$) δ = -59.65. HRMS: (ESI+) Calculated for $C_{15}H_{11}F_6N_4S^+$: 393.0603, Found: 393.0606.

### *4-(Dimethylamino)benzaldehyde 4-(3,5-Bistrifluoromethylphenyl)thiosemicarbazone (1g):*

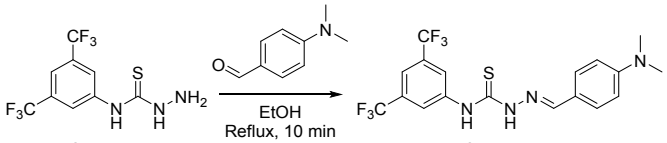


1 1g

Thiosemicarbazide **1** (758 mg, 2.50 mmol) was dissolved in ethanol (96 %, 10 mL) and 4-(dimethylamino)benzaldehyde (0.56 g, 3.75 mmol) was added. While stirring, the reaction mixture was heated until boiling and approximately half of the volume was allowed to evaporate. The reaction mixture was cooled in an ice-bath, and the off-white precipitate was collected and air-dried. Yield: 952 mg (88 %).

Melting Point: 195 – 200 °C (dec.). Elemental analysis for $C_{18}H_{16}F_6N_4S$: Found (calculated) 49.90 % C (49.77); 3.40 % H (3.71), 12.80 % N (12.90). $^1$H NMR (500 MHz, DMSO-$d_6$) δ = 11.97 (s, 1H), 10.35 (s, 1H), 8.53 (s, 2H), 8.09 (s, 1H), 7.85 (s, 1H), 7.72 (d, *J*=9.0, 2H), 6.74 (d, *J*=9.0, 2H), 2.98 (s, 6H). $^{13}$C NMR (126 MHz, DMSO-$d_6$) δ = 174.43, 151.74, 145.31, 141.24, 129.68 (d, *J*=32.9), 129.29, 124.83, 123.30 (q, *J*=272.7), 120.71, 117.42, 111.57, 39.72. $^{19}$F NMR (282 MHz, DMSO-$d_6$) δ = -59.75. HRMS: (ESI+) Calculated for $C_{18}H_{17}F_6N_4S^+$: 435.1073, found: 435.1062.

### *4-(Methoxycarbonyl)benzaldehyde 4-(3,5-Bistrifluoromethylphenyl)thiosemicarbazone (1h):*

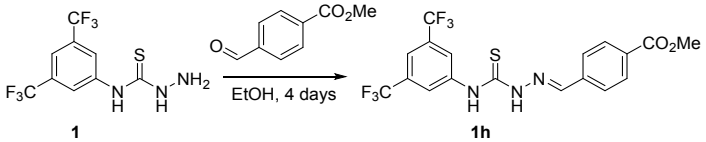


1 1h

Thiosemicarbazide **1** (152 mg, 0.50 mmol) was dissolved in ethanol (96 %, 2 mL) and 4-(methoxycarbonyl)benzaldehyde (123 mg, 0.75 mmol) was added. The reaction mixture was stirred for four days before it was cooled in a freezer (ca. -15 °C), and the white precipitate was collected and air-dried. Yield: 189 mg (84 %).

Melting Point: 216 – 219 °C. Elemental analysis for $C_{18}H_{13}F_6N_3O_2S$: Found (calculated) 48.31 % C (48.11), 2.68 % H (2.92), 9.27 % N (9.35). $^1$H NMR (500 MHz, DMSO-$d_6$) δ = 12.36 (s, 1H), 10.59 (s, 1H), 8.46 (s, 2H), 8.27 (s, 1H), 8.07 (d, *J*=8.3, 2H), 8.01 (d, *J*=8.3, 2H), 7.92 (s, 1H), 3.87 (s, 3H). $^{13}$C NMR (126 MHz, DMSO-$d_6$) δ = 176.16, 165.82, 142.81, 140.97, 138.18, 130.60, 129.81 (q, *J*=33.0), 129.41, 127.92, 125.64, 123.25 (q, *J*=272.7), 118.17, 52.30. $^{19}$F NMR (282 MHz, DMSO-$d_6$) δ = -59.73. HRMS: (ESI+) Calculated for $C_{18}H_{14}F_6N_3O_2S^+$: 450.0705, Found: 450.0701.

### *4-Cyanobenzaldehyde 4-(3,5-Bistrifluoromethylphenyl)thiosemicarbazone (1i):*

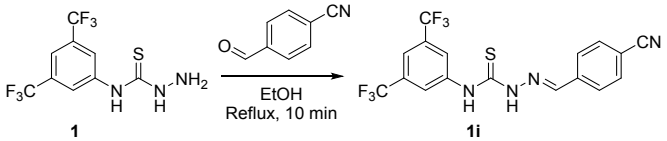


Thiosemicarbazide **1** (152 mg, 0.50 mmol) was dissolved in ethanol (96 %, 2 mL) and 4-cyanobenzaldehyde (98.3 mg, 0.75 mmol) was added. While stirring, the reaction mixture was heated until boiling and approximately half of the volume was allowed to evaporate. The reaction mixture was cooled in a freezer (ca. -15 °C), and the white precipitate was collected, recrystallized from ethanol (96 %, ca. 1 mL) and air-dried. Yield: 94.1 mg (45 %).

Melting Point: 222 – 225 °C (dec.). Elemental analysis for $C_{17}H_{10}F_6N_4S$: Found (calculated) 49.23 % C (49.04); 2.12 % H (2.42), 13.32 % N (13.46). $^1$H NMR (500 MHz, DMSO-$d_6$) δ = 12.42 (s, 1H), 10.61 (s, 1H), 8.45 (s, 2H), 8.24 (s, 1H), 8.14 (d, *J*=7.9, 2H), 7.97 – 7.87 (m, 3H). $^{13}$C NMR (126 MHz, DMSO-$d_6$) δ = 176.27, 142.05, 140.91, 138.22, 132.56, 129.84 (q, *J*=33.1), 128.33, 125.69, 123.23 (q, *J*=272.7), 118.71, 118.26, 112.05. $^{19}$F NMR (282 MHz, DMSO-$d_6$) δ = -59.65. HRMS: (ESI+) Calculated for $C_{17}H_{11}F_6N_4S^+$: 417.0603, found: 417.0599.

### *4-(Trifluoromethyl)benzaldehyde 4-(3,5-Bistrifluoromethylphenyl)thiosemicarbazone (1j):*

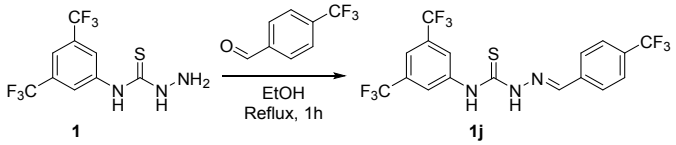


Thiosemicarbazide **1** (96.0 mg, 0.32 mmol) was dissolved in ethanol (96 %, 1.5 mL) and 4-(trifluoromethyl)benzaldehyde (0.1 mL, 0.8 mmol) was added. While stirring, the reaction mixture was heated until boiling and approximately half of the volume was allowed to evaporate. The reaction mixture was cooled in a freezer (ca. -15 °C), and the white precipitate was collected and air-dried. Yield: 19.1 mg (13 %).

Melting Point: 163 – 165 °C. Elemental analysis for $C_{17}H_{10}F_9N_3S$: Found (calculated) 44.73 % C (44.45); 1.90 % H (2.19), 9.04 % N (9.15). $^1$H NMR (500 MHz, $CDCl_3$) δ = 9.33 (bs, 1H), 9.31 (bs, 1H), 8.28 (s, 2H), 7.91 (s, 1H), 7.83 (d, *J*=8.2, 2H), 7.75 (s, 1H), 7.73 (d, *J*=8.2, 2H). $^{13}$C NMR (126 MHz, $CDCl_3$) δ = 191.23, 176.06, 141.72, 139.28, 135.88, 132.33 (q, *J*=33.7), 130.07, 127.93, 126.29 – 126.16 (m), 123.14 (q, *J*=272.4), 119.62, 117.55. $^{19}$F NMR (282 MHz, $CDCl_3$) δ = -61.73 (6F), -61.78 (3F). HRMS: (ESI+) Calculated for $C_{17}H_{11}F_9N_3S^+$: 460.0524, found: 460.0532.

### *4-Bromobenzaldehyde 4-(3,5-Bistrifluoromethylphenyl)thiosemicarbazone (1k):*

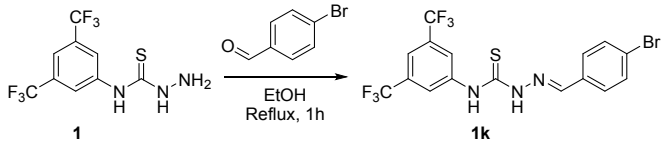


4-Bromobenzaldehyde (92.5 mg, 0.50 mmol) was dissolved in ethanol (96%, 2 mL) and thiosemicarbazide **1** (152 mg, 0.50 mmol) was added. While stirring, the reaction mixture was heated until boiling and approximately half of the volume was allowed to evaporate. The remainder of the solvent was removed by drying under a stream of nitrogen and the remaining solid was recrystallized from ethyl acetate (ca. 2 mL) to give a light yellow powder that was air-dried. Yield: 62.6 mg (27 %).

Melting Point: 190 – 192 °C. Elemental analysis for $C_{16}H_{10}BrF_6N_3S$: Found (calculated) 41.14 % C (40.87), 2.01 % H (2.14), 8.90 % N (8.94). $^1$H NMR (500 MHz, DMSO-$d_6$) δ = 12.26 (s, 1H), 10.52 (s, 1H), 8.46 (s, 2H), 8.17 (s, 1H), 7.90 (s, 1H), 7.89 (d, *J*=8.5, 2H), 7.66 (d, *J*=8.5, 2H). $^{13}$C NMR (126 MHz, DMSO-$d_6$) δ = 175.91, 143.01, 141.01, 133.00, 131.71, 129.81 (q, *J*=33.2), 129.69, 125.51, 123.73, 123.26 (q, *J*=272.7), 118.06. $^{19}$F NMR (282 MHz, $CDCl_3$) δ = -61.72. HRMS: (ESI+) Calculated for $C_{16}H_{11}BrF_6N_3S^+$: 469.9756, Found: 469.9777.

### *4-tert-Butylbenzaldehyde 4-(3,5-Bistrifluoromethylphenyl)thiosemicarbazone (1l):*

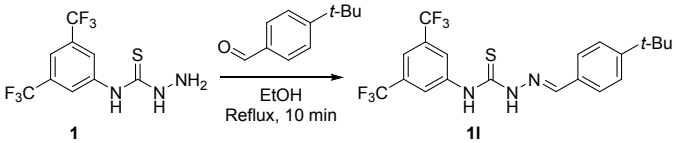


Thiosemicarbazide **1** (152 mg, 0.50 mmol) was dissolved in ethanol (96 %, 2 mL) and 4-*tert*-butylbenzaldehyde (0.13 mL, 0.75 mmol) was added. While stirring, the reaction mixture was heated until boiling and approximately half of the volume was allowed to evaporate. The reaction mixture was cooled in a freezer (ca. -15 °C), and the white precipitate was collected and air-dried. Yield: 162 mg (72 %).

Melting Point: 201 – 202 °C. Elemental analysis for $C_{20}H_{19}F_6N_3S$: Found (calculated) 53.84 % C (53.69), 3.99 % H (4.28), 9.32 % N (9.39). $^1$H NMR (500 MHz, $CDCl_3$) δ = 9.45 (s, 1H), 9.40 (s, 1H), 8.29 (s, 2H), 7.89 (s, 1H), 7.72 (s, 1H), 7.64 (d, *J*=8.5, 2H), 7.48 (d, *J*=8.5, 2H), 1.35 (s, 9H). $^{13}$C NMR (126 MHz, $CDCl_3$) δ = 175.59, 155.23, 144.12, 139.53, 132.21 (q, *J*=33.7), 129.76, 127.68, 126.23, 123.76, 123.19 (q, *J*=272.8), 119.26, 35.23, 31.27. $^{19}$F NMR (282 MHz, $CDCl_3$) δ = -61.80. HRMS: (ESI+) Calculated for $C_{20}H_{20}F_6N_3S^+$: 448.1277, Found: 448.1276.

## *4-Methoxybenzaldehyde 4-(3,5-Bistrifluoromethylphenyl)thiosemicarbazone (1m):*

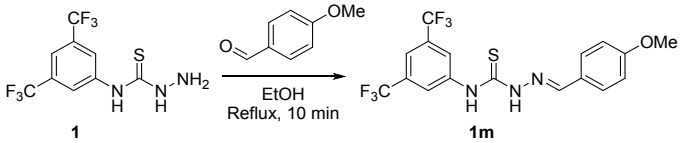


Thiosemicarbazide **1** (152 mg, 0.50 mmol) was dissolved in ethanol (96 %, 2 mL) and 4-methoxybenzaldehyde (0.1 mL, 0.8 mmol) was added. While stirring, the reaction mixture was heated until boiling and approximately half of the volume was allowed to evaporate. The reaction mixture was cooled in a freezer (ca. -15 °C), and the white precipitate was collected and air-dried. Yield: 147 mg (70 %).

Melting Point: 165 – 168 °C. Elemental analysis for $C_{17}H_{13}F_6N_3OS$: Found (calculated) 48.28 % C (48.46), 2.88 % H (3.11), 9.87 % N (9.97). $^1$H NMR (500 MHz, $CDCl_3$) δ = 9.37 (s, 2H), 8.28 (s, 2H), 7.86 (s, 1H), 7.72 (s, 1H), 7.66 (d, *J*=8.7, 2H), 6.97 (d, *J*=8.8, 2H), 3.87 (s, 3H). $^{13}$C NMR (126 MHz, $CDCl_3$) δ = 175.13, 162.10, 143.78, 139.31, 131.93 (q, *J*=33.9), 129.31, 124.85, 123.51, 122.94 (q, *J*=272.9), 118.97, 114.48, 55.39. $^{19}$F NMR (282 MHz, $CDCl_3$) δ = -61.71. HRMS: (ESI+) Calculated for $C_{17}H_{14}F_6N_3OS^+$: 422.0756, Found: 422.0753.

## *4-(4-Butylphenyl)thiosemicarbazide (3):*

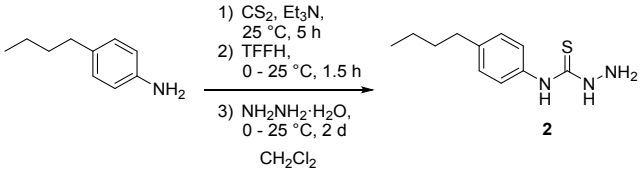


4-Butylaniline (1.58 mL, 10 mmol) was dissolved in $CH_2Cl_2$ (20 mL) and triethylamine (2.77 mL, 20 mmol) and $CS_2$ (1.22 mL, 20 mmol) was added. The solution was stirred at room temperature for five hours, before it was cooled on an ice-bath and TFFH (2.64 g, 10 mmol) was added. After the addition, the ice-bath was removed and the solution was stirred for 1.5 hours at room temperature. Once again the solution was cooled on an ice-bath and hydrazine-hydrate (50 – 60 %, 5 mL, 0.1 mol) was added carefully over five minutes. The ice-bath was removed and the solution was stirred for two days at room temperature before it was quenched with water (50 mL). The aqueous phase was extracted with ethyl acetate (3 x 50 mL) and the combined organic phases were backwashed once with water (50 mL) before they were dried ($Na_2SO_4$) and concentrated *in vacuo*. The crude product was recrystallized from ethanol and air-dried to yield 1.62 g (73 %) of white crystals.

Melting point: 113 – 115 °C. Elemental analysis for $C_{11}H_{17}N_3S$: Found (calculated) 59.45 % C (59.16); 7.54 % H (7.67); 18.89 % N (18.81). $^1$H NMR (500 MHz, $CDCl_3$) δ = 9.15 (bs, 1H), 7.94 (bs, 1H), 7.52 – 7.33 (m, 2H), 7.24 – 7.12 (m, 2H), 3.97 (bs, 2H), 2.63 – 2.56 (m, 2H), 1.62 – 1.54 (m, 2H), 1.40 – 1.30 (m, 2H), 0.95 – 0.90 (m, 3H). $^{13}$C NMR (126 MHz, $CDCl_3$) δ 180.14, 129.61, 128.98, 125.53, 124.52, 35.28, 33.65, 22.46, 14.07. HRMS: (ESI+) Calculated for $C_{11}H_{18}N_3S^+$: 224.1216, found: 224.1213.

## *Benzaldehyde 4-(4-Butylphenyl)thiosemicarbazone (3a):*

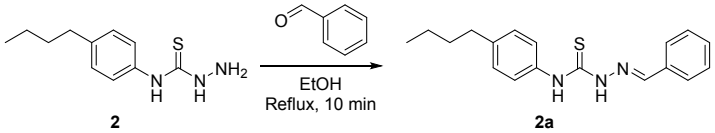


Thiosemicarbazide **2** (223 mg, 1.00 mmol) was dissolved in ethanol (96 %, 4 mL) and benzaldehyde (0.51 mL, 5 eq.) was added. While stirring, the reaction was heated until the solvent was boiling. Approximately half of the volume was allowed to evaporate before the reaction mixture was cooled in an ice-bath, and the precipitate was collected and recrystallized from boiling ethanol (96 %, 1 mL). Yield: 277 mg (89 %).

Melting point: 158 – 159 °C. Elemental analysis for $C_{18}H_{21}N_3S$: Found (calculated) 69.47 % C (69.42); 6.63 % H (6.80); 13.47 % N (13.49). $^1$H NMR (500 MHz, $CDCl_3$) δ = 9.82 (s, 1H), 9.14 (s, 1H), 7.91 (s, 1H), 7.70 – 7.65 (m, 2H), 7.55 (d, *J*=8.3, 2H), 7.44 – 7.40 (m, 3H), 7.22 (d, *J*=8.2, 2H), 2.63 (t, *J*=7.7, 2H), 1.66 – 1.58 (m, 2H), 1.43 – 1.33 (m, 2H), 0.94 (t, *J*=7.3, 3H). $^{13}$C NMR (126 MHz, $CDCl_3$) δ 176.09, 142.85, 141.33, 135.46, 133.18, 130.85, 129.06, 128.92, 127.59, 124.72, 35.36, 33.66, 22.50, 14.10. HRMS: (ESI+) Calculated for $C_{18}H_{22}N_3S^+$: 312.1529, found: 312.1537.

### *3,5-Bis(trifluoromethyl)benzaldehyde 4-(4-Butylphenyl)thiosemicarbazone (3b):*

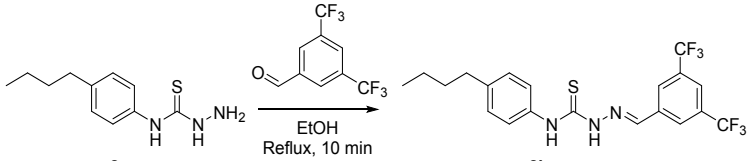


2 2b

Thiosemicarbazide **2** (223 mg, 1.00 mmol) was dissolved in ethanol (96 %, 4 mL) and 3,5-bis(trifluoromethyl)benzaldehyde (164 µL, 1.05 mmol) was added. While stirring, the reaction was heated until the solvent was boiling. Approximately half of the volume was allowed to evaporate before the reaction mixture was cooled in an ice-bath, and the precipitate was collected and recrystallized from boiling ethanol (96 %, 1 mL). Yield: 447 mg (95 %).

Melting point: 199 – 200 °C. Elemental analysis for $C_{20}H_{19}F_6N_3S$: Found (calculated): 53.81 % C (53.59); 3.99 % H (4.28); 9.37 % N (9.39). $^1$H NMR (500 MHz, $CDCl_3$) δ = 10.53 (s, 1H), 9.06 (s, 1H), 8.09 (s, 2H), 8.04 (s, 1H), 7.90 (s, 1H), 7.52 (d, *J*=8.3, 2H), 7.26 (d, *J*=8.3, 2H), 2.65 (t, *J*=7.8, 2H), 1.66 – 1.59 (m, 2H), 1.44 – 1.32 (m, 2H), 0.94 (t, *J*=7.4, 3H). $^{13}$C NMR (126 MHz, $CDCl_3$) δ 176.44, 142.07, 139.32, 135.47, 134.98, 132.66 (q, *J*=33.8), 129.11, 127.13 (d, *J*=4.3), 125.27, 123.77, 123.08 (q, *J*=273.0), 35.39, 33.63, 22.50, 14.09. $^{19}$F NMR (282 MHz, $CDCl_3$) δ -61.85. HRMS: (ESI+) Calculated for $C_{20}H_{20}F_6N_3S^+$: 448.1277, found: 448.1286.

### *Bis(3,5-bis[trifluoromethyl]phenyl) Thiourea (Schreiner's catalyst, 4):*

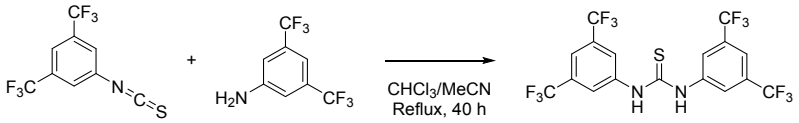


4

3,5-Bis(trifluoromethyl)aniline (165 mg, 0.718 mmol, 1.2 eq.) was dissolved in $CHCl_3$ (5.0 mL) and 3,5-bis(trifluoromethyl)phenyl isothiocyanate (163 mg, 0.601 mmol, 1.0 eq.) was added via syringe. Acetonitrile (2.0 mL) was added and the resulting clear solution was heated under reflux for 40 hours after which all of the solvent was removed under reduced pressure. The white residue was recrystallized from boiling chloroform (9 mL) to yield the title compound as white needles. Yield: 292 mg (97 %).

Melting point: 174 – 175 °C (lit.: 172 – 173 °C).[12] Elemental analysis for $C_{17}H_8F_{12}N_2S$: Found (calculated) 41.15 % C (40.81), 1.48 % H (1.61), 5.60 % N (5.60). $^1$H NMR (500 MHz, DMSO) δ = 10.64 (s, 2H), 8.20 (s, 4H), 7.87 (s, 2H). $^{13}$C NMR (126 MHz, DMSO) δ = 180.59, 141.15, 130.34 (q, *J*=32.7), 124.16, 123.16 (q, *J*=272.3), 117.79. $^{19}$F NMR (282 MHz, DMSO) δ = -59.77. HRMS: (ESI+) Calculated for $C_{17}H_9F_{12}N_2S^+$: 501.0289, found: 501.0291.

[12] Y.-B. Huang and C. Cai, *J. Chem. Res.*, 2009, 686.